

Computational Modeling and Forensic Analysis for Terrorist Airplane Bombing: a Case Study

Jean Yeh¹, Goong Chen^{1, 2}, Cong Gu³, James “Tom” Thurman⁴, Alexey Sergeev¹, Chunqiu Wei⁵, Jing Zhu⁶, Hichem Hajaiej⁷, Ying-Feng Shang⁸, Feng Zhu⁹ and M. Tahir Mustafa¹⁰

¹Department of Mathematics, Texas A&M University, College Station, TX 77843, USA.

²Institute for Quantum Science and Engineering, Texas A&M University, College Station, TX 77843, USA

³Keysight Technologies, 1400 Fountaingrove Parkway, Santa Rosa, CA 95403, USA

⁴School of Safety, Security and Emergency Management, Eastern Kentucky University, Richmond, KY 40475

⁵School of Mathematics and Statistics, Beijing Institute of Technology, Liangxiang University Town, Fangshan District, Beijing, China

⁶School of Mathematics and Statistics, University of Science and Technology Beijing, Beijing, China

⁷Department of Mathematics, California State University at Los Angeles, 5151 State University Dr., Los Angeles, CA 90032, USA

⁸School of Mathematics, Tianjin University, Tianjin, China

⁹School of Mathematics and Applied Mathematics, Jiangsu University, Zhenjiang, Jiangsu, China

¹⁰Department of Mathematics, Statistics and Physics, Qatar University, P.O. Box 2713, Doha, Qatar

Abstract

The bombing of airliners has been a tactic used by terrorists during the past 40 years. Its prevention is a major priority by homeland security officials on a worldwide basis. In efforts to aid in the investigation of such bombings, this paper provides the results of the development of mathematical modeling and computer simulation for the study of aircraft bombings and associated forensics. As an assist in the forensic study, a number of photographs are provided to depict the normally observed physical characteristics of explosives damage upon aircraft and related materials. Our study illuminates and evaluates how these characteristics can be captured by computational mechanics. Finally, we use the laptop bombing of Daallo Airlines Flight 159 as a case study to demonstrate that event reconstruction can be accomplished for the purpose of forensic investigations. Most of our supercomputer results are visualized by video animations in order to show the dynamic effects and phenomena of explosives and the associated event reconstruction.

Keywords: Explosives, airplane bombing, fracture and damage, computational modeling and simulation, forensics, event reconstruction.

1 Introduction

This paper studies the computational mechanics and forensics of fracture, damage and destruction of passenger airliners by the detonation of explosives.

One tactic used by terrorists is the bombing of airliners, especially large aircraft. Such bombings have resulted in extensive causalities in addition to the loss of the aircraft, and caused damage and loss of lives on the ground. In fact, much of todays palpable homeland security anti-terrorism measures have placed great emphasis on the prevention of bombings of passenger airliners through heightened airport inspection procedures. Logically, such measures have, to a large extent, successfully prevented potential airplane bombings. As a consequence, civil aviation remains the safest among all modes of travel.

Still, major issues regarding airplane bombings stand at the forefront of homeland security studies. Such issues pertain to, e.g., mechanical designs of airframes and baggage containers that can withstand the explosives effects of a bomb of a limited size, post explosion forensics and investigation as well as others. Specifically, this study evaluates the problem of airliner bombings from a large-scale scientific computation and simulation perspective in order to gain knowledge about what to physically expect in such an event. Clearly, these issues are the motivational factors for this research depicted in this study and in the analysis of the Daallo Airlines Flight 159 bombing on February 2, 2016, near Mogadishu, Somalia, Africa.

By its very nature, the study of airliner bombings is complex, requiring a team of investigators with various skill sets and a protracted time-period to conduct the investigation. This largely explains why this paper involves multi-authorships as listed. Because of the complex geometric shapes of the airframe and supporting structures, analytical and theoretical studies generally can provide only insights or results of the heuristic and qualitative nature. Alternatively, experimental studies can provide the real-thing but are hampered by excessive costs of setup and the challenges of overpressure measurements due to fast detonation dynamics. In comparison, computer modeling and simulation can provide high quality visualization (i.e., observation) and fidelity without the high cost and, therefore, offer an excellent alternative approach to this problem.

Explosives damage and the resulting destruction of an airframe are normally the end results of the fracture processes initially caused by the high intensity shock wave and other particles from the detonation of the improvised device. Depending on the relative altitude of the airplane at the time of the explosion, its destruction can be completed with the rapid, explosive (mechanical) decompression of the airframe. At a fundamental level, this is essentially a study of the effects of blast impacts on metal. In this connection, it is a well studied subject (see [1, 2], for example). However, such knowledge is hardly sufficient when it comes to airplane bombings because airliners have special geometric shapes and internal supporting structures. These, in fact, are the most distinguishing features of this study, and may explain why there have been few public research articles in the literature on the effects of bombings on aircraft. This subject matter, in some sense, is also taboo because terrorists could very well take advantage of such knowledge for their vile purposes.

Here, our objectives are mainly forensic in order to understand the following *through*

phenomenology and visualization:

- (i) the effectiveness of computational mechanics in capturing blast phenomena;
- (ii) the destructive effects to airframes by detonation according to the varying amounts of explosives;
- (iii) the damage to the aircraft in the specific incident of Daallo Airlines Flight 159 referred to earlier.

Items (i) and (ii) above offers a *general treatment* for airliner bombings, while item (iii) treats a *specific case/example*. We hope their study has covered a lot of ground in both generality and specificity as far as airplane bombings are concerned. It is understood that the topical field is extensive and additional manpower and efforts are needed in order to develop a more comprehensive theory.

This paper is organized as follows:

- (i) Section 2 displays a photo set manifesting major characteristics of blast phenomena intended as goals to be reached and matched by computational work.
- (ii) In Section 3, we will describe the essential modeling aspects, tabulating the fundamental physical and empirical laws and numerical methods that constitute the basis for computer modeling based on the software tool LS-DYNA. Validation is also given.
- (iii) In Section 4, we will compute and then visualize general explosive and destructive effects of bombings on an airplane or a metal plate and compare results with those in Section 2.
- (iv) In Sections 5 , we will address the modeling, computation and simulation of the laptop bombing case of the Daallo Airlines Flight 159 case, (This Section is mainly based on the work done in the PhD Dissertation of Jean Yeh [3], the first author, at Texas A&M University under the advisement of G. Chen.)
- (v) Section 6 offers some final comments and forward-looking statements.

Our ultimate objective is that through the systematic, methodological development of our work here, one now can have the basic capability to actually computationally test old and new aircraft designs and materials which can withstand bombing/blast effects better for future higher crashworthiness and survivability in a terrorist attack or airplane accident (such as the explosion of the jet fuel tank). Hopefully, this work will attract the attention of and pave the way for both industry and individual researchers to further contribute to this important direction.

2 Phenomenology of Bombing: A Set of Must-Know Characteristics for a Real-World Postblast Investigation

The detonation/explosion of a high explosive (e.g., dynamite, TNT, RDX, PETN, C-4, among others) produces rapidly expanding hot gases propagating at supersonic speeds which, if present, can have a devastating effect on a constraining structure. Cracks, fractures and structural collapse ensue according to the various viscoplasticity properties of the materials and leave many postblast footprints that can provide unmistakable signatures for forensic investigations.

One of the coauthors, J.T. Thurman, has more than 40 years of applied experience in the U.S. Army and the FBI doing bomb disposal and forensic investigation of bombing incidents. In his book [4], he has listed a number of observable characteristics for the examination, analysis, differentiation, tracking, and event reconstruction of postblast investigation. The major findings among them are the following material evidences and patterns at the scene, illustrated by Figures 2.1 - 2.5:

- (P1)** The bending and rolling of metal onto/under itself; cf. Figure 2.1;
- (P2)** The jaggedness along the edges; cf. Figures 2.2;
- (P3)** Small cratering and micro-pitting on the surface; cf. Figure 2.3;
- (P4)** The thinning and feathering on the edge; cf. Figure 2.4;
- (P5)** The blackening on the damage-surface; cf. Figure 2.5.

Some of the photos are taken from the bombing tragedy of the Pan Am Flight 103 occurring on December 21, 1988, where 243 passengers and 16 crew, plus 11 people on the ground for total of 270 were killed [5, 6].

metal bent-inward

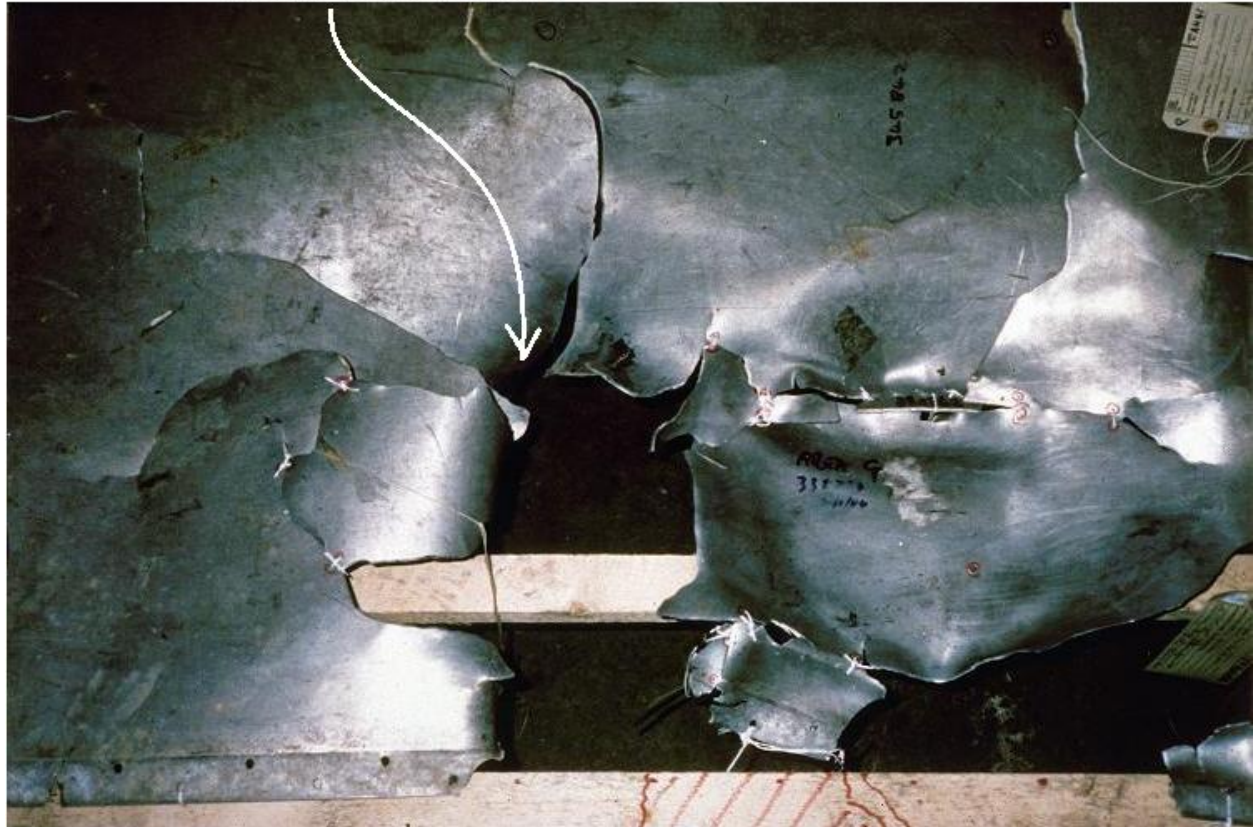
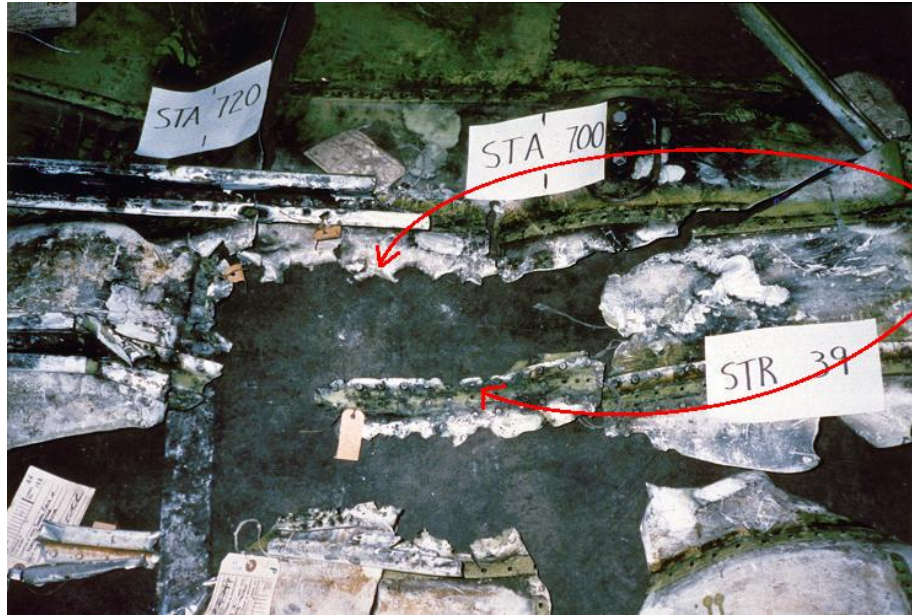
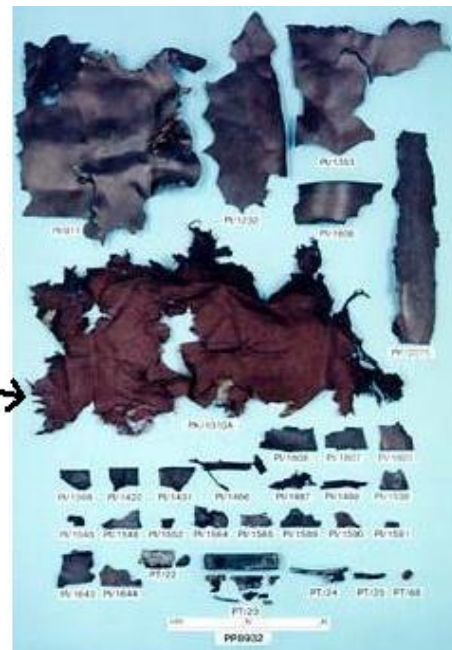


Figure 2.1: **Photo for (P1)**. We can see that the metal is bent and rolled onto/under itself in a directional-coherent pattern. In this photo, blast damage done onto a sheet of metal is observable wherein the metal/target material was protected by something else and the forces/pressure “punched” a hole through it. The many pieces of bent metal are indicative of the direction of explosion and thereby can point to the placement of the explosives and the epicenter of explosion to form what would be a “tube-like” cone. Here please note that none of these metal fragments have actually rolled onto themselves. However, in the computer simulations in subsequent sections, we can see such “complete rolling onto selves” if the detonation force is strong.



jaggedness



(b)

Figure 2.2: **Photo for (P2).** (a) It shows the *jaggedness* of the metal fragments. It comes from the reconstruction phase of the bombed Pan Am Flight 103. A distinctive pattern has emerged. Notice in the center (explosion epicenter) of the photo that all of the severed ends of the skin metal fragments are jagged, not smooth. This is explosive's damage. Now direct your attention to the radiating lines extending outward from the epicenter of the explosion. These are tears in the metal resulting from the rapid decompression of the aircraft, in other words – mechanical damage. These are *not* characteristics of explosives damage. (b) It shows the recovered remains of a suitcase from Pan Am Flight 103, wherein a high energy high explosive was contained therein. Please note the varying fragment sizes and the *jaggedness* of the edges. Along the edges one can also see the “blackening” of some of the components. Thus, even for fabrics and plastics (that are non-metallic), the jaggedness and blackening patterns are observable.

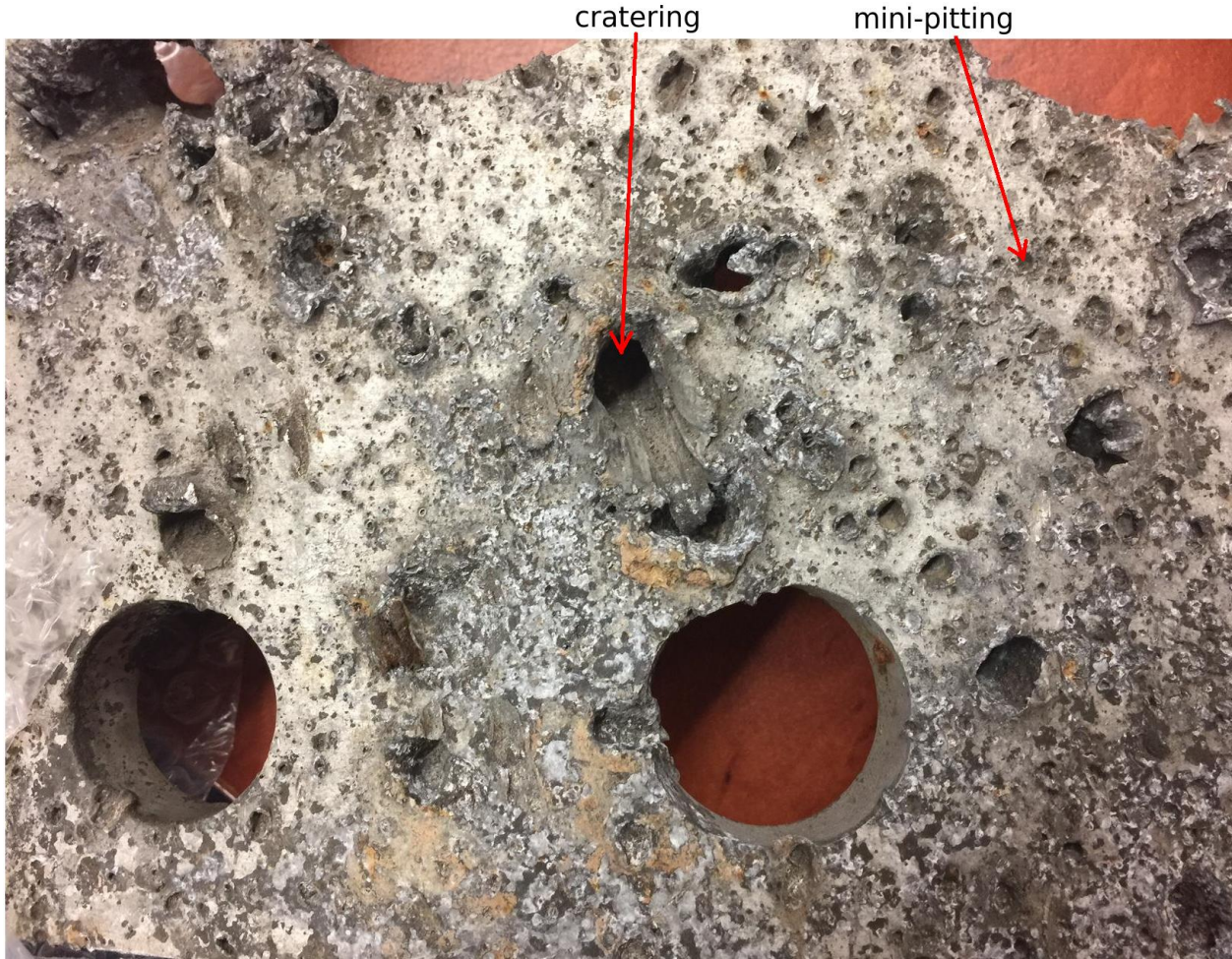


Figure 2.3: **Photo for (P3)**. It shows “pitting and cratering”. This is characteristic of being in close contact with the detonation of a high energy high explosive. One may note that some of the holes (other than the manufactured holes) are larger than others as well as deeper. There are numerous “micro-pittings” due to the impact of hot gases resulting from the combustion (detonation) of the explosives with the metal.



Figure 2.4: **Photo for (P4).** It is an example of “thinning and feathering”. Essentially, due to the excessive forces and the stretching from the explosion, the metal is made thinner, pretty much like taking a rolling pin and rolling out bread dough! Note the sharp edges of the metal and various degrees of thinning, with some more than others.

blackened surface

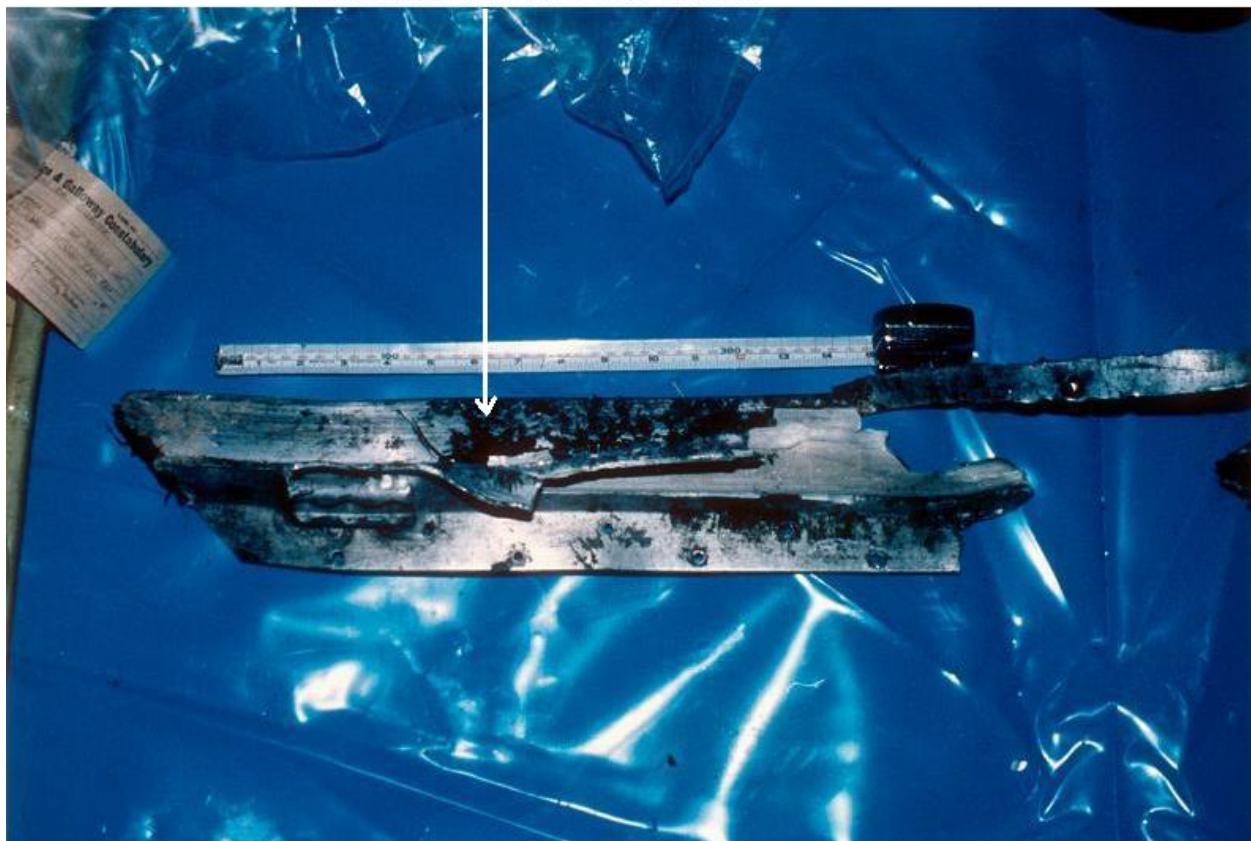


Figure 2.5: **Photo for (P5).** One can observe the “blackening” on this metal fragment. This is the result of “gas washing” from the combustion (detonation) of the explosive onto the material. Essentially, the combustion of the ingredients of the explosive is instantly converted into a shock wave containing reacted and unreacted materials. When these materials impact with “target materials”, they can become impinged on them, thereby appearing to be a black, oil-like stain. This can be observed in many, but not all explosions and is a good place to conduct explosives residue swabbings. (As a side note: airframes are notoriously dirty and many of the components will be black and discolored from other causes than explosive’s damage.)

How many of these patterns as bombing characteristics, (P1) - (P5), and how well *they can be captured by computational mechanics* for forensic purposes? These will constitute the goalposts for our computational study to reach and match; see Section 4, in particular, Table 4.1.

3 Computer Modeling of Airplane Bombing Based on LS-DYNA, and Validation

For the study of a complex, fast-reacting dynamical process such as the bombing of an airliner, analytical (closed form) solutions are impossible and can't be expected. Experimental measurements are challenging to make as the process is abrupt and destructive, with high cost. Therefore, *computational mechanics* becomes a preferred methodology. As the computations involve *explosions, solid mechanics* and *fracture*, the most established, reputed tool in these fields is *LS-DYNA*. It is the computer modeling software developed by the Livermore Software Corporation [7] with over forty years of development history. It is our tool of choice for mathematical and computer modeling throughout the paper.

3.1 Compact Outlines of Mathematical and Computer Modeling

The mathematical and computer modeling of our study of interest is divided into two parts: the mathematical modeling based on LS-DYNA, and the computer simulation implemented on the supercomputer. The essentials of these two parts are described compactly in, respectively, Boxes 1 and 2 in the following.

Box 1 Mathematical model for bombing based on LS-DYNA

Software
LS-DYNA

Spatial domain

A region in \mathbb{R}^3 with high explosive (HE) within a metal confinement (such as airplane).

Governing equations

For air: the standard system of conservation equations of mass, momentum, and energy. These lead to the compressible Navier-Stokes and the associated energy equations for the gaseous fluid (air).

For solid (metallic) confinement: viscoplasticity model of solid MAT_PLASTIC_KINEMATIC is selected in LS-DYNA [8, Manual Vol II, p.2-95]

For HE: the material model MAT_HIGH_EXPLOSIVE_BURN is chosen from LS-DYNA [8, Manual Vol II, p.2-110]

Empirical relations

The Jones-Wilkins-Lee equation of state (EOS_JWL in LS-DYNA [8, Manual Vol II, p.1-18])

$$p = A \left(1 - \frac{\omega}{R_1 V} \right) e^{-R_1 V} + B \left(1 - \frac{\omega}{R_2 V} \right) e^{-R_2 V} + \frac{\omega E}{V},$$

is used for the relationship in air-blast between pressure (p), volume (V) and energy (E), with experimental parameters A, B, R_1, R_2 and ω (cf., for example, Table 3.3).

The Cowper and Symonds model

$$\frac{\sigma_y}{\sigma_0} = 1 + \frac{\dot{\epsilon}}{C}^{1/p}$$

is chosen for the strain rate for the aircraft skin in LS-DYNA [8, manual Vol II, p.2-96], [8, Theory Manual, p.19.15]

The Johnson and Cook model expressing the flow stress as

$$\sigma_y = (A + B\bar{\epsilon}^p^n)(1 + C \ln \dot{\epsilon}^*)$$

is used for the aircraft stations, where A, B are the hardness constant, n is the hardness exponent, C is the strain rate constant (see Table 3.2), $\bar{\epsilon}^p$ is effective plastic strain and $\dot{\epsilon}^*$ is normalized effective strain rate.

Mathematical methods for discretization

The finite element method for metal/solids, and smoothed particle hydrodynamics (SPH) for blast particles. Spatial discretization uses the finite element method, while time discretization uses explicit finite difference.

Impact-Contact conditions

The impact between the blast SPH nodes and the metal/aircraft body is modeled by CONTACT_AUTOMATIC_NODES_TO_SURFACE in LS-DYNA [8, Manual Vol I, p.11-2], while the contact force between various fragments is modeled by CONTACT_ERODING_SINGLE_SURFACE [8, Manual Vol I, p.11-51].

Fracture criteria

According to LS-DYNA [8, Theory Manual, p.18.15]

- $p \geq p_{min}$ where P is the pressure (positive in compression), and p_{min} is the pressure at failure.
- $\sigma_1 \geq \sigma'_{max}$, where σ_1 is the maximum principal stress, and σ_{max} is the principal stress at failure..
- $\sqrt{\frac{3}{2}\sigma'_{ij}\sigma'_{ij}} \geq \bar{\sigma}_{max}$, where σ'_{ij} are the deviatoric stress components, and $\bar{\sigma}_{max}$ is the equivalent stress at failure.

- $\epsilon_1 \geq \epsilon_{max}$, where ϵ_1 is the maximum principal strain, and ϵ_{max} is the principal strain at failure.
- $\gamma_1 \geq \gamma_{max}$ where γ_1 is the shear strain, and γ_{max} is the shear strain at failure.
- The Tuler-Butcher criterion,

$$\int_0^t [\max(0, \sigma_1 - \sigma_0)]^2 dt \geq K_f,$$

where γ_1 is the maximum principal stress, γ_0 is a specified threshold stress, $\sigma_1 \geq \sigma_0 \geq 0$, and K_f is the stress impulse for failure. Stress values below the threshold value are too low to cause fracture even for very long duration loadings. (Only *macroscopic*, not microscopic, fractures are considered in this paper.)

Merging of two materials

For the merging of two different materials (such as, for example, an acrylic-made window, with the metal body of an airplane fuselage), we choose `CONTACT_TIED_SURFACE_TO_SURFACE_FAILURE` or `CONTACT_TIEBREAK_SURFACE_TO_SURFACE_ONLY` in LS-DYNA [8, Manual Vol I, p.11-58].

Pressure difference between the exterior and the interior of the confinement

We use `LOAD` in LS-DYNA [8, Manual Vol I, p.27-1] to load the pressure difference (*8 psi*) between inside and outside of the aircraft on the skin of the aircraft.

Initial conditions

All the blast initial conditions are assumed to be *stationary*.

Parameters for confinement-material

To be specified as each individual case is being treated; some are given below in Box 1, while other example are given elsewhere.

Parameters	Aluminum 7075-T6	Plastic	Acrylic
Density (kg/m^3)	3000	1400	1200
Young's modulus (GPa)	70	1.4	3.2
Poisson's ratio	0.35	0.39	0.37
Yield stress (GPa)	0.47	0.016	0.071

Table 3.1: Parameters used in `MAT_PLASTIC_KINEMATIC`. Aluminum alloy 7075-T6 is used for the aircraft skin, plastic is used for the passenger cabin and acrylic is used for the windows.

Parameters for Aluminum 2024	Value
Density (kg/m^3)	2770
Young's modulus (GPa)	70
Poisson's ratio	0.33
Hardness constant A (GPa)	0.265
Hardness constant B (GPa)	0.426
Hardness exponent n	0.41
Strain Rate Constant C	0.01

Table 3.2: Parameters for Aluminum alloy 2024 used for the aircraft stations by MAT_SIMPLIFIED_JOHNSON_COOK

Parameters for high explosives (HE)

In this paper, only two HE are used: TNT and C-4. Their material parameters are given in Table 3.3.

Parameters for HE	TNT	C-4
Density	1630 kg/m^3	1601 kg/m^3
Detonation velocity	6930 m/s	8193 m/s
Chapman-Jouget pressure	21 GPa	28 GPa
A in JWL	371.2 GPa	609.7999 GPa
B in JWL	2.23 GPa	13 GPa
R_1 in JWL	4.15	4.5
R_2 in JWL	0.95	1.4
ω in JWL	0.3	0.25
Initial E in JWL	7 GJ/m^3	9 GJ/m^3
Initial V in JWL	1.0	1.0

Table 3.3: Parameters for high explosives TNT and C-4 in the JWL equation.

End of Box 1

The implementation of Box 1 (whether with LS-DYNA or other software) often engenders a large scale system that requires the use of supercomputers. This type of computer-simulation work is synonymously called *computer modeling (CM)*. Box 2 delineates the several standard, key procedures for *CM*. Note that some steps in Box 2 are mutually interactive with the methodologies given in Box 1.

Box 2 Computer modeling procedures	
CM1: Preprocessing	model selections, choice of proper physical and computational parameters, grid generations. (One can use LS-PREPOST [9] for grid generation if <i>LS-DYNA</i> software is chosen.)
CM2: Computing/ supercomputing	code development, algorithm designs, implementation on a supercomputer.
CM3: Postprocessing	representation of numerical output data in terms of graphics, tables or animation videos. (One can use LS-POST [9] for video animation and visualization if <i>LS-DYNA</i> is used. Our most favored video animation tool is the third-party product ParaView [10]. ParaView has ray-tracing capability that captures optical effects with movie-like quality. Nevertheless, it's a lengthy process to convert the supercomputer output data format to the one for Paraview, often requiring several days on the supercomputer.)
CM4: Validation	comparison and confirmation between computed data and experimental data.

By implementing Boxes 1 and 2 on the ADA supercomputer at Texas A & M University's High Performance Research Computing Center, we have computed numerous cases of airplane bombing. But we must first demonstrate that our numerical work is well validated. This is presented in the next subsection.

3.2 Validation of Blast Simulation

Validation is an important, indispensable part of any scientific computation. No calculations can be deemed correct and complete without testing and confirming with experimental data. Nevertheless, for the bombing examples considered above, after a diligent search of literature, we have not been able to find any similar experimental examples doing blast on aluminum alloy samples to yield recorded data as benchmarks for validation. The closest example we have found is the study from the report by Shirey [11] that does blasting of steel plates. We now validate our SPH blast computational modeling approach by mimicking Shirey's explosion test. The test was used to investigate the breach of a steel plate after a direct explosion by the high energy explosive C-4 molded into the shape of circular disks; see Figure 3.1 for the set-up, and Figure 3.2 for the simulation processes. Shirey concluded that there is a threshold of explosive thickness needed for breaching the plate. If the diameter of the explosive disk is small, it needs to be thicker in order to breach the steel plate. However, when the diameter is large enough, there is a minimum thickness requirement to breach the steel plate. (See the red curve in Figure 3.3 for this property). Since Shirey didn't provide specific details of the material properties of the steel used in the test, we have decided to

choose some common steel and experimented with *failure strains* values of 0.28, 0.31 and 0.41. For these three values of failure strains, one of the simulation results, curve (a) in Figure 3.3 shows qualitatively a good match. Figure 3.3 shows the thresholds of explosive thickness from both the LS-DYNA simulations and Shirey's experiment. The material model for the steel plate part is **MAT_PLASTIC_KINEMATIC**, and we used **MAT_HIGH_EXPLOSIVE_BURN** for the C-4 explosive. See the parameters in Table 3.3 and Table 3.4.

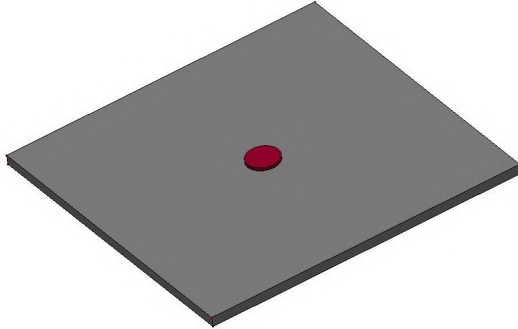


Figure 3.1: Explosive set-up geometry for Shirey's explosion test. A cylindrical shaped C-4 explosive is placed upon a 6 mm steel plate.

Parameters	Values
Density	7691 kg/m^3
Young's modulus	210 GPa
Poisson's ratio	0.3
Yield stress	0.3 GPa

Table 3.4: Parameters for steel plate.

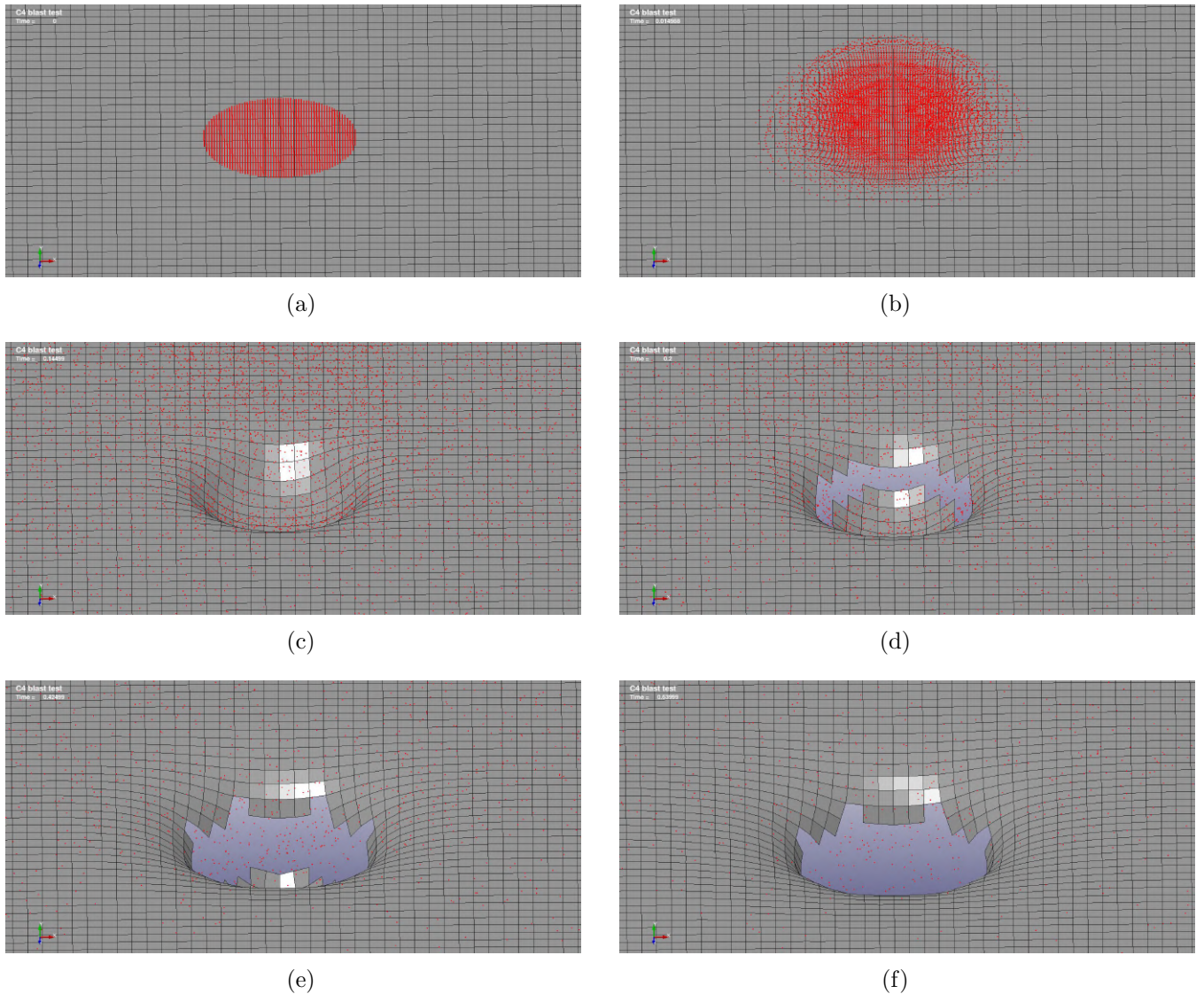
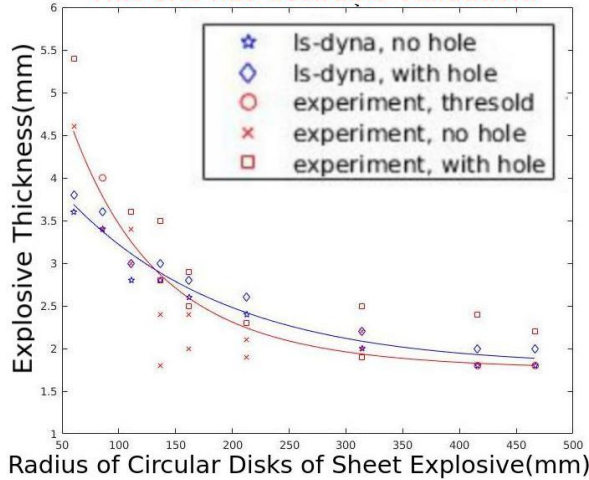


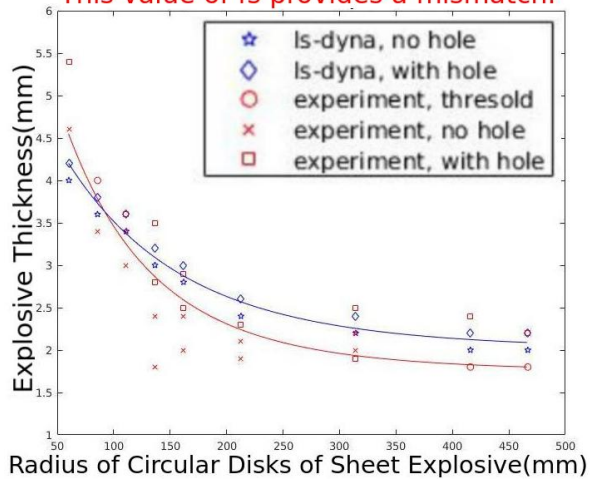
Figure 3.2: Snapshots of simulation for Shirey's explosion test. The demonstrated case used a C-4 explosive charge with radius 60.32 mm and thickness 4.8 mm. The steel plate is meshed with cell size 10 mm \times 10 mm. See our video animation in <http://goo.gl/dUJQtw>

C4 test, 6mm steel plate, $fs=0.28$
This one has desirable validation.



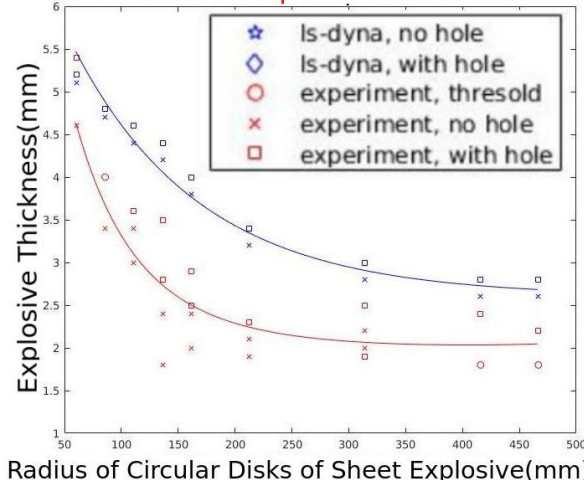
(a)

C4 test, 6mm steel plate, $fs=0.31$
This value of fs provides a mismatch.



(b)

C4 test, 6mm steel plate, $fs=0.41$
This value of fs provides a mismatch.



(c)

Figure 3.3: Threshold curves for 6 mm steel plate with three different value of failure strains. The curve in (a) show a good qualitative match with the value 0.28 for the failure strain. This serves as desirable validation. Note that the matches in (b) and (c) are poor, due to the mis-chosen values of fs

Jasak, et al's book [1] contains blast tests on reinforced concrete structures done by Forsen [2] and Lonnqvist [12]. They concluded that the diameter of the blast hole satisfies an affine-linear relationship; see Figure 3.4. We did not conduct the numerical simulations of these for reinforced concrete. However, we point out that our numerical simulations for the explosion on aircraft fuselage also shows an affine-linear relationship between explosive charge weight and hole diameter; cf. Figure 3.5.

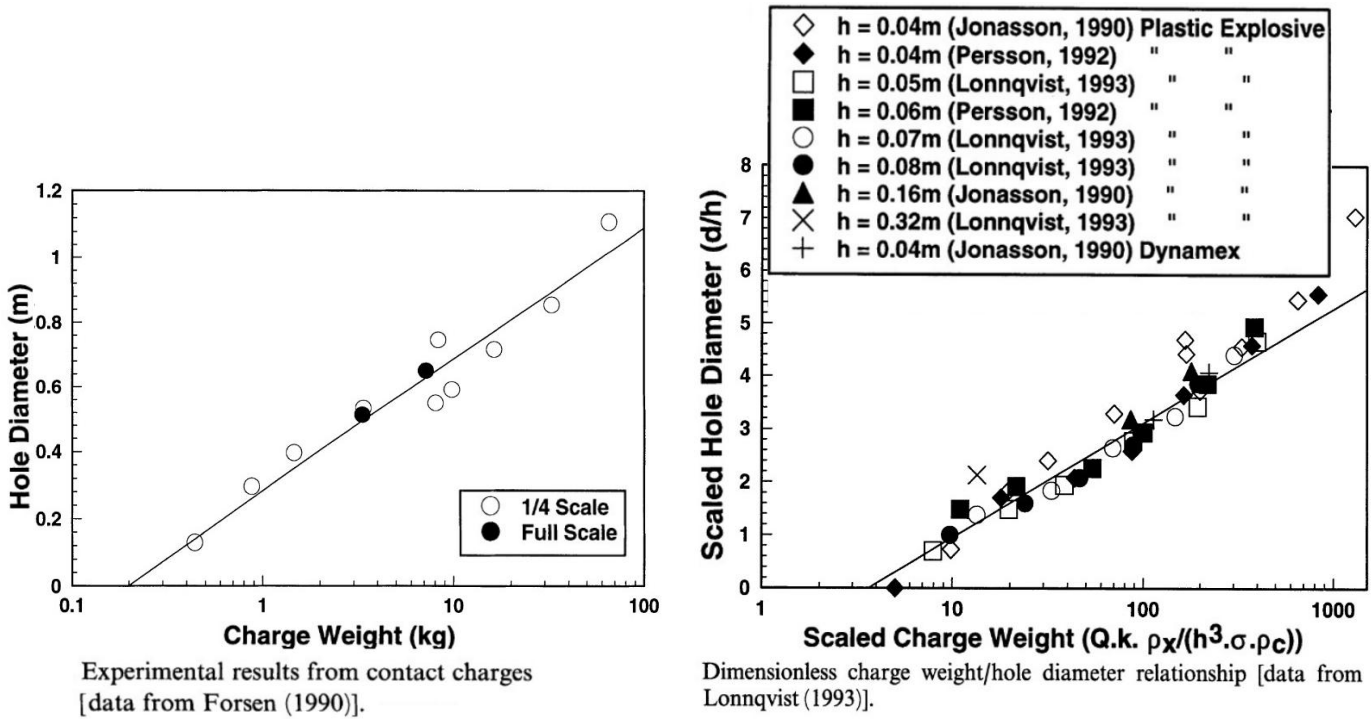


Figure 3.4: Relationship between explosive charge weight and hole diameter for reinforced concrete explosive test; from Jasak, et al work, available in [1]

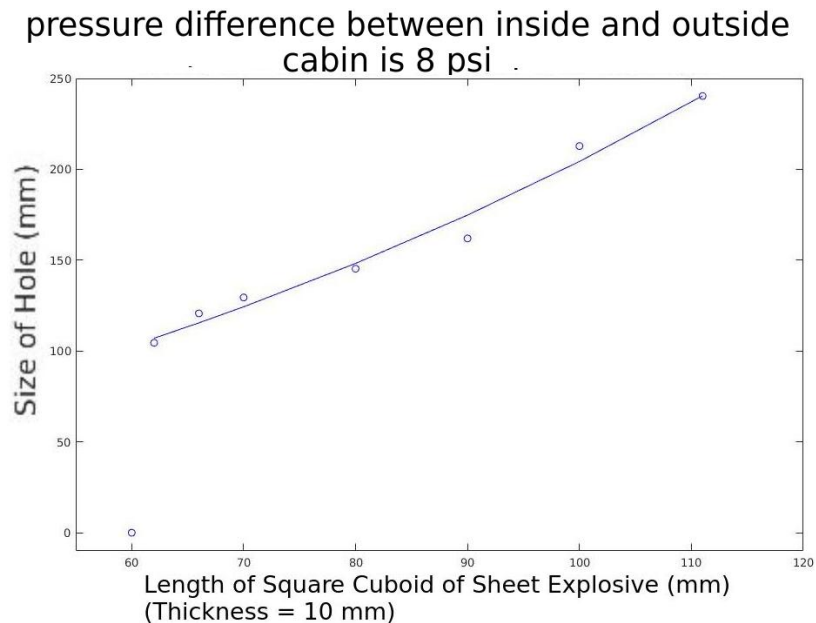


Figure 3.5: Relationship between explosive charge weight and hole diameter in aircraft explosion.

As noted earlier, we have not found in the open literature about specific details of metal-

blasts dedicated solely for the purpose of benchmarking and validation – Shirey’s explosion test [11] is the only one we have found that is closest to our interest. But our numerical results shown in the three graphics in Figure 3.3 clearly indicate the importance of choosing a *right value for failure strains*.

4 Aircraft Blast Simulations and Phenomena

This section serves two purposes:

1. we want to see the dramatic effects of the dynamic display of demolition of an airframe by large amounts of explosives;
2. we check how well computational mechanics can capture the major characteristics, (P1) - (P5), of blast phenomena as outlined in Section 2 and manifested in the various photos therein.

A mid-section airframe similar to that of Boeing 737, containing stringer, aluminum skin, supporting stations, and fastened with rivets, was made by “Simon” [13] using CATIA 3D CAD/CAM rendering software [14], which was downloaded from GrabCAD website [13]. This section of fuselage has mass 1369 kg. We use LS-PREPOST [9] to generate mesh. See Figure 4.1.

We consider three cases.

Case 1: Explosion from inside

The explosive is shaped as a ball inside the fuselage, with its center placed at coordinates (0,0,2841)(in units of mm). In Figure 4.2, the mass of the TNT explosive is chosen to be 106.76 kg. See the video animation, made from several perspectives, as given in the URL in the captions of Figure 4.2.

Case 2: Explosion from outside

This Case is similar to **Case 1**, except that the ball-shaped explosive charge is placed *outside* the airframe, centered at the location (2300,160,2450). The separation between the airframe and the charge is 20 mm. The amount of TNT explosive is also the same. See Figure 4.3 and the video animation given in the captions of Figure 4.3.

Case 3: Explosion from inside with varying amounts of explosives The above **Cases 1 and 2** were computed with a large amount of explosives (106.76 kg) in order to manifest dramatic explosion effects. Here, we vary the amounts of explosives to be 200 kg, 50 kg, 25 kg and 12.5 kg in mass and visualize the explosion and damage process side by side. See Figure 4.4 and the video animation given in its captions.

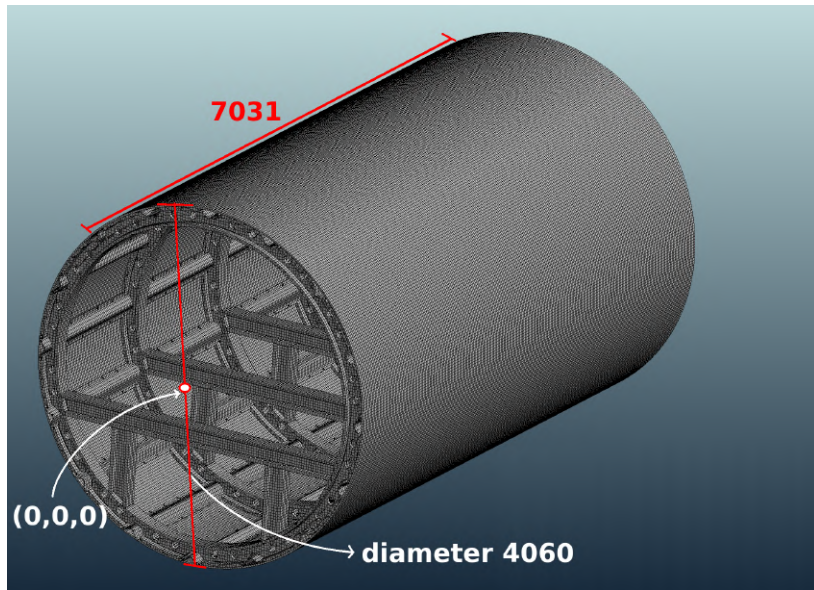


Figure 4.1: The airframe configuration (made by “Simon”) is taken from [13]. We use LS-PREPOST to generate mesh as shown. The mesh has 406781 nodes and 393255 faces. The diameter is 4060, the length 7031 (in units of mm), and the origin of the coordinate system is indicated.

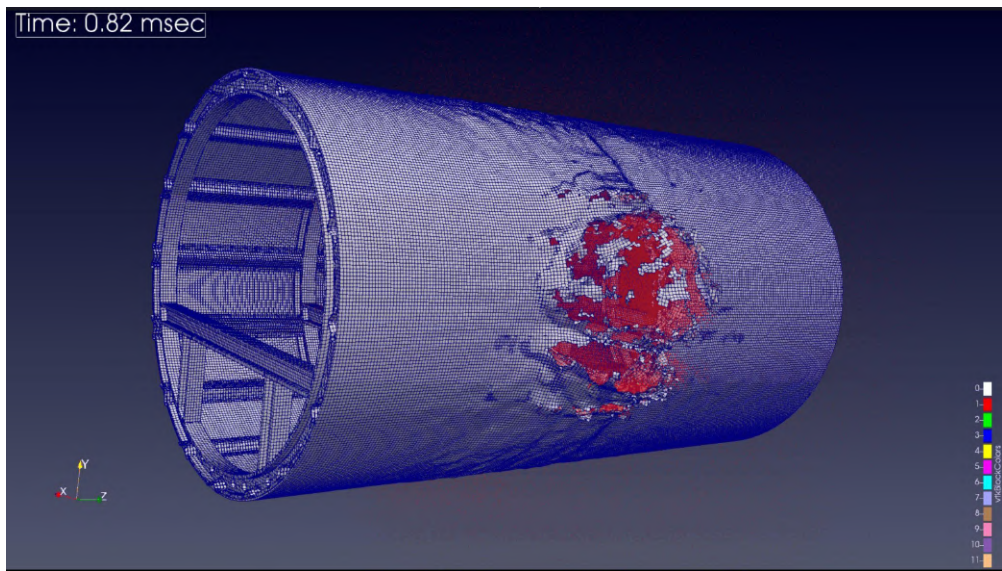


Figure 4.2: A ball-shaped explosive charge of diameter 495 mm with center at coordinates (1550,160,2450) is placed in the interior of the airframe. The amount of TNT used is 106.76 kg. The separation between the airframe and the charge is 223 mm. It is then detonated. Several view-points, frontal/side/oblique, and a semitransparent presentation, are shown; see the video animation at <https://www.dropbox.com/s/22legz1zuuzy5bz/inside-new.mp4>

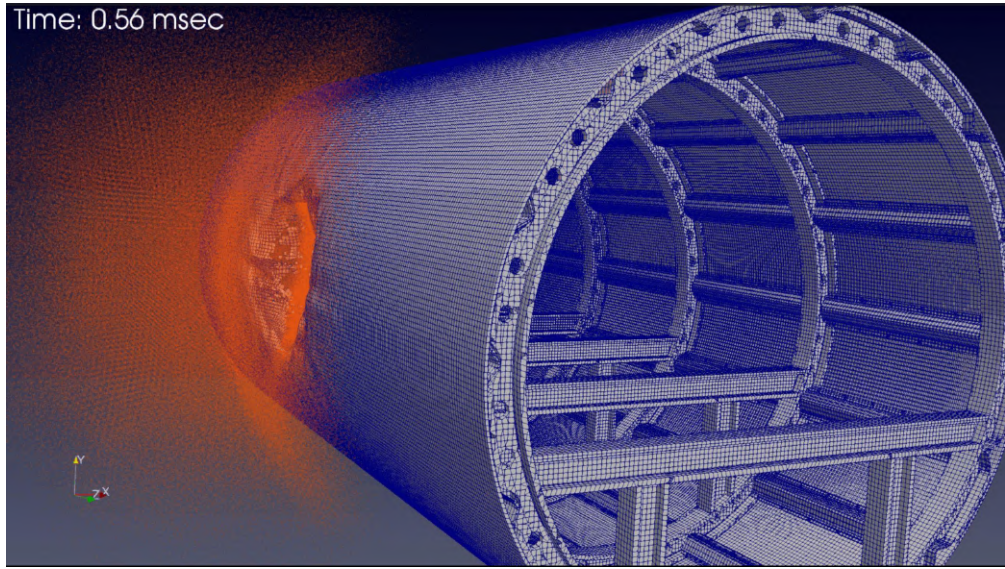


Figure 4.3: A ball-shaped explosive charge with center at coordinates (2300,160,2450) is placed in the exterior point close to the airframe. The amount of TNT used is 106.76 kg. The separation between the airframe and the charge is 20 mm. It is then detonated. Several view-points, outside/inside/cross-sectional, are shown; see the video animation at <https://www.dropbox.com/s/38bbpxohsfmkm9w/outside-new.mp4>

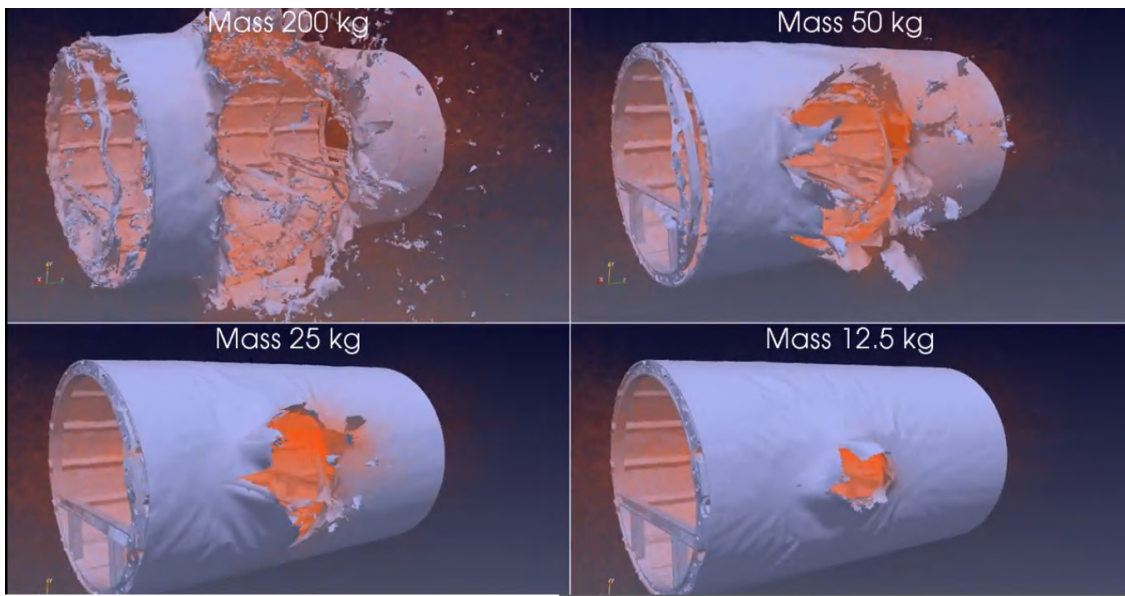


Figure 4.4: A panel of four explosions, using explosive amounts of 200 kg, 50 kg, 25 kg and 12.5 kg, is displayed side-by-side in order to view and compare the effects of damage; see the video animation at <https://www.dropbox.com/s/0dwckao778bjef9/3-panels-comparison-c.avi>

After the visualizations in Figures and videos in Figures 4.2 through 4.4, it is now clear that *the bombing characteristics (P1) in Section 2*, namely the bending and rolling of metal onto/under itself is conspicuous. Some of the fragments and large chunks of debris are illustrated in Figure 4.5.

Next, the explosion characteristics (P2) from Section 2, namely, the *jaggedness along the rim of fragments* are examined.

Returning to the Validation Subsection 3.2, we use the breaching test of steel plate to demonstrate jaggedness along the rim of fracture. For the steel plate with thickness 6 mm, we use LS-PREPOST to generate a uniform mesh of cell size $10 \text{ mm} \times 10 \text{ mm}$ of rectangular 2D finite elements and then breach it by detonating varying amounts of C-4 explosive. Then as Figure 4.5(a) has illustrated, the rim of the cratered hole does not show a strong pattern of jaggedness. Obviously, *there is a lack of sufficient resolution for jaggedness to happen*. However, after refining the mesh up to the one-hundredth (i.e., 1%) scale of the diameter of the cratered hole in the neighborhood of the hole, the pattern of jaggedness has emerged, as can be seen from Figure 4.6(b). *Therefore, in order for computational outcomes to successfully capture the pattern of jaggedness, the mesh must have sufficient resolution*.

Next, the third bombing characteristics, (P3), the pitting and cratering on the surface of fragments are examined. As can be seen in Figure 2.3's photo, many of the pittings on a surface are caused by high speed impact of hot gases of reacted materials as well as unreacted debris. Thus, they can be of rather fine scale. In Figure 4.7, we show that our computations are able to capture some of the larger pittings/craterings. However, *for the great majority of those of the fine-scale, the computer simulation is not capable of capturing this (P3) phenomenon*. Again, the fineness of the spatial resolution plays an important role - much more so than the preceding case for (P2) here.

Now, the thinning and feathering along the edges of fragments of the computational outcomes are examined. In order to make this investigation somewhat easier, we assume that the steel plate is a little thicker with thickness 10 mm (versus 6 mm in the computational case of Figure 4.6). In the video animation given in the captions of Figure 4.8, one can clearly see that as the bomb is exploding, the cratering process is causing a *stretch of the metal and, therefore, is making it thinner*. We can see a peak thinning of about 30% of thickness from Figure 4.8(a). This helps our understanding as to why thinning happens. Nevertheless, at the end of the blast, when we examine the crater edge, the sharpening/thinning/feathering pattern is not strong; see Figure 4.8(b).

Finally, we examine the phenomenon (P5), the blackening of the damage-surface. This blackening is caused by reacted and unreacted micro-particles impacting and then adhering to the surface. It will require a *highly fine scale resolution* to capture this phenomenon, if at all possible.

We summarize our “audit” of the computational methodology and outcomes in capturing the five important characteristics of postblast phenomena in Table 4.1.

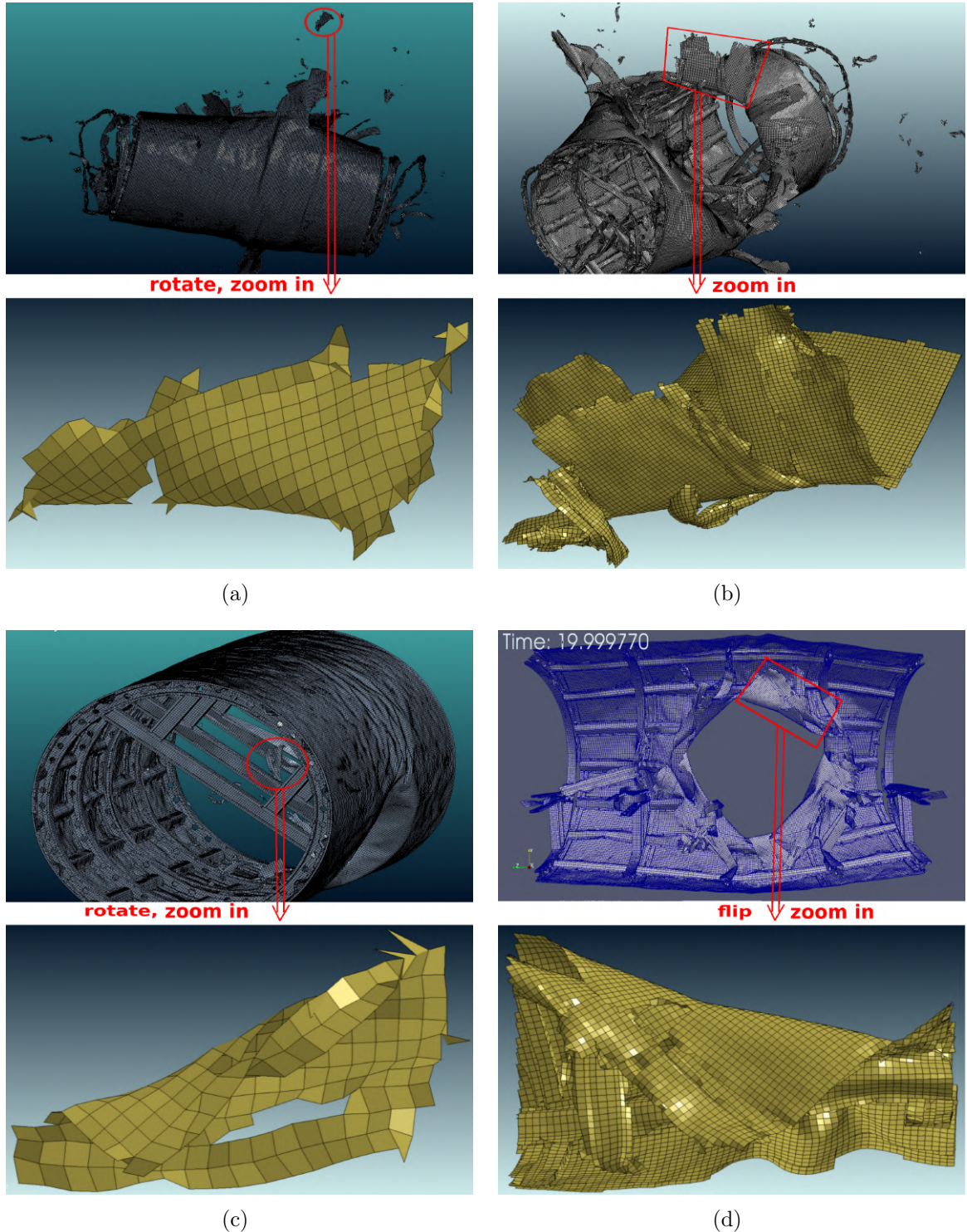


Figure 4.5: Samples of fragments and bent parts of debris from the explosions computed in Figures 4.2 (parts (a) and (b)) and 4.3 (parts (c) and (d)). One can see that with large explosions, metal can bend $\pm 180^\circ$.

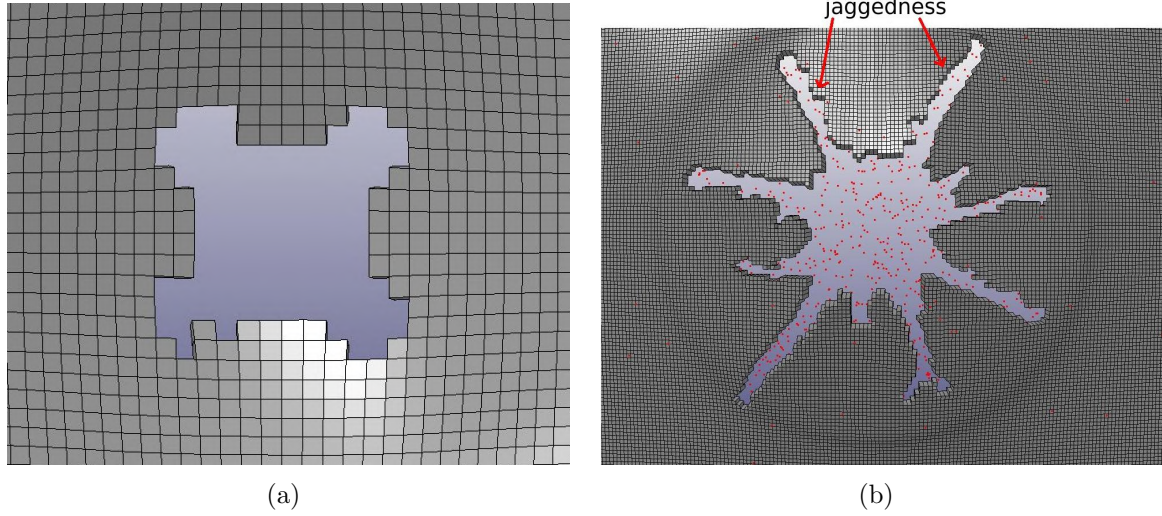


Figure 4.6: In this blast test, the amount of explosive charge C-4 used is 0.56 kg (cylinder with radius 136.52 mm and thickness 6 mm), on a 6 mm steel plate. Panel (a) has a crude mesh, with cell size $10 \text{ mm} \times 10 \text{ mm}$, and the resulting hole shows essentially no pattern of jaggedness. Panel (b) has a much finer resolution (cell size $2.5 \text{ mm} \times 2.5 \text{ mm}$) near the crater, and the jaggedness along the rim of the is conspicuous. For video animation, see <http://goo.gl/fnvjhM>

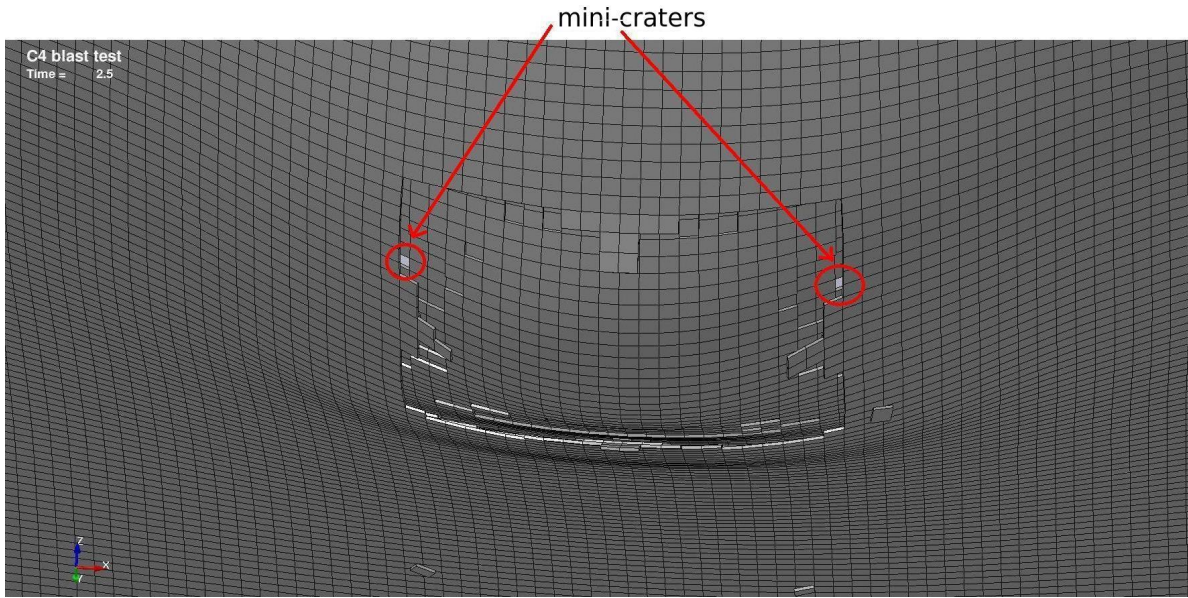
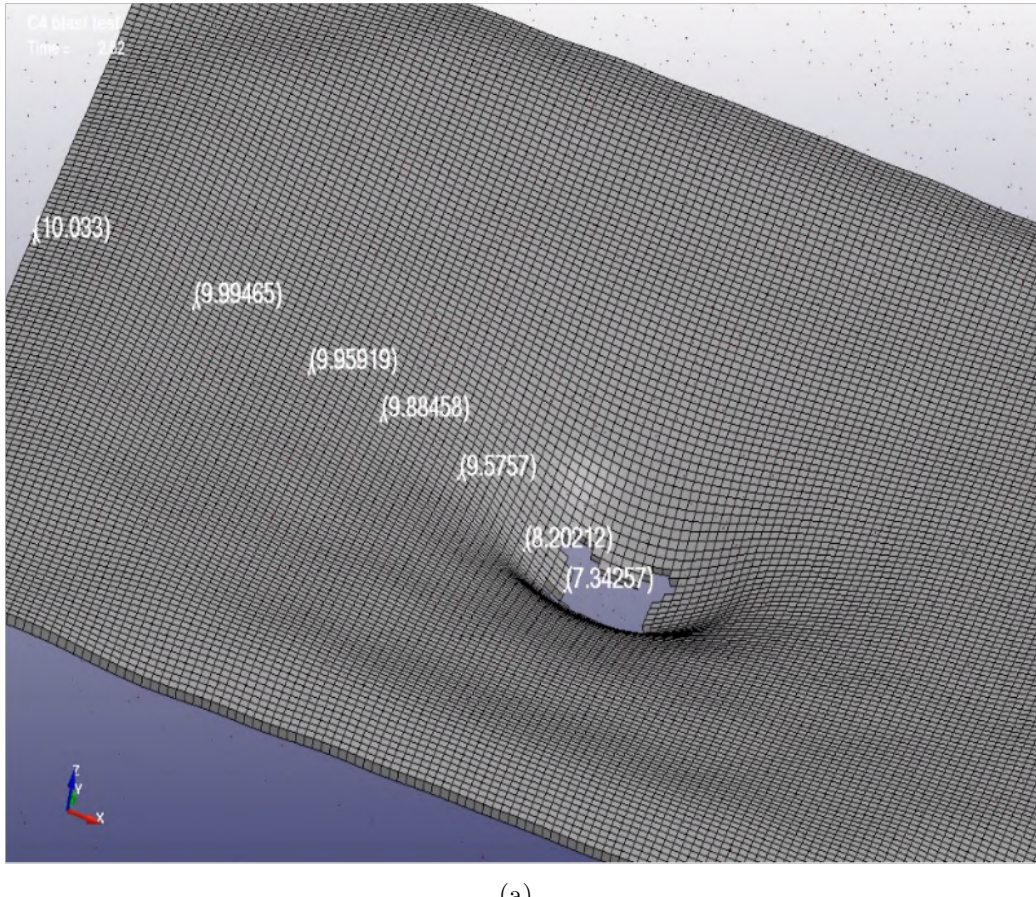
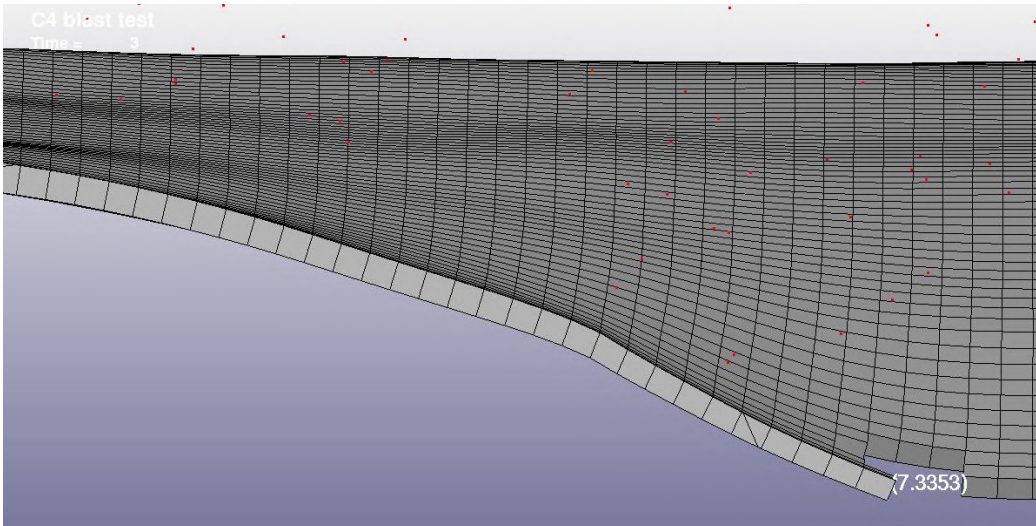


Figure 4.7: This figure shows some small-scale cratering as indicated on the steel plate in the process of being breached. See the video animation in <http://goo.gl/EMYH5L>



(a)



(b)

Figure 4.8: This figure is intended to test the thinning and feathering along the edges of blast breaching of a steel metal plate, with thickness 10 mm. In part (a), we see that as cratering is in progress, the plate is stretched and this causes the reduction of thickness as indicated by the thickness indicators in the figure. In part (b), at the end of the blast, nevertheless, we do not see the emergence of a sharp edge as shown in Figure 2.4, even though the thickness has been reduced to 7.33 mm (from 10 mm).

Bombing characteristics			Computer simulation results	
Types	Properties	Photos	Graphics and videos	satisfactory degree of capturing bombing characteristics
(P1)	bending and rolling onto self	Fig. 2.1	Figs. 4.2, 4.3, 4.4, 4.5	high
(P2)	jaggedness pattern along the rim	Figs. 2.2	Fig. 4.6	reasonably high if sufficient spatial resolution is introduced
(P3)	small cratering and micro-pitting	Fig. 2.3	Fig. 4.7	low
(P4)	thinning and feathering along the edge	Fig. 2.4	Fig. 4.8	low
(P5)	blackening of damage surface	Fig. 2.5	none	not possible so far

Table 4.1: “Performance audit” of computer simulation in the capturing of bombing characteristics (P1)-(P5).

The blast computations in this section used large amounts of explosives in order to illustrate the dramatic effects. In actual terrorist plots, the amount of explosives will be much smaller. We will provide a contrast case in the following section (where only a small amount of explosives is used) as a concrete example for our case study.

5 Case Study of the Daallo Airlines Flight 159 Laptop Bombing

Thankfully, airliner incidents, regardless of the cause happen at rather infrequent time intervals. Here we select a most recent incident as a case study, namely, the laptop bombing of Daallo Airlines Flight 159 occurring on February 2, 2016. A terrorist retrofitted a laptop computer, inserted explosives, passed the security system at Aden Adde (Mogadishu) International Airport, Somalia, and boarded the said flight destined for Djibouti, Africa. At the altitude of 11,000 feet, the bomb exploded, blowing a large hole on the fuselage. The alleged bomber got sucked out of the airplane through the hole caused by the explosion, with his dead body being recovered on the ground in the town of Dhiqaaley near Balad, Somalia. Consequently, this bombing had a profound ripple effect for the airline traveling public. On March 21, the US and UK banned laptop carry-ons on flights of nine airlines originating from North Africa and Mideast. (This ban was controversial, so it was lifted after four months.)

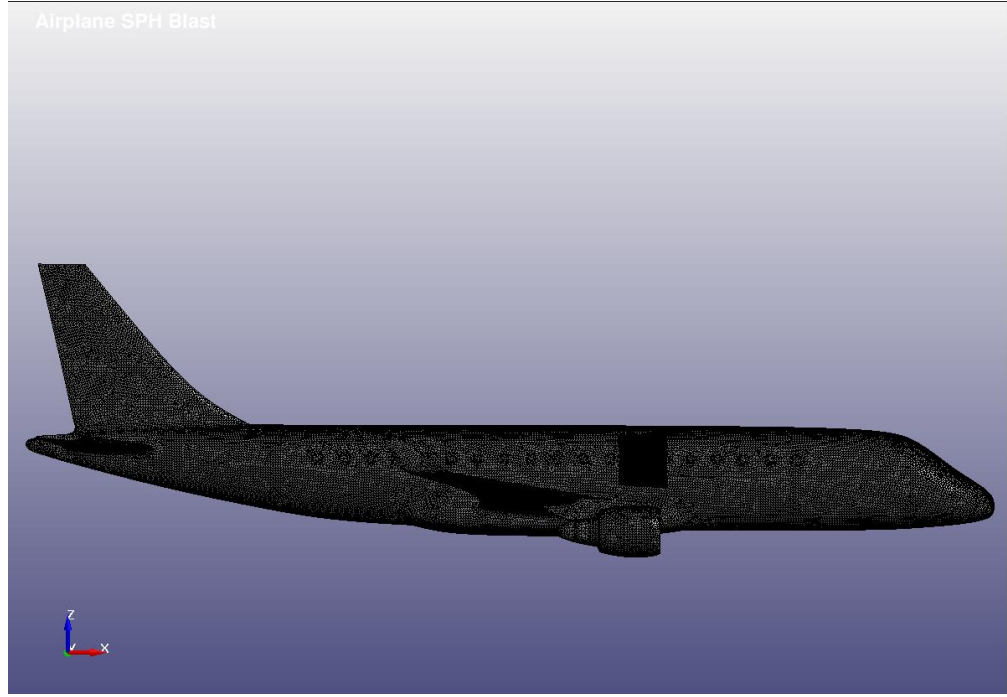
Even though Flight 159 experienced a bombing, it was able to survive and safely return to the originating airport where the damage was assessed with little mystery involved as to its cause. This instance provided an excellent case for the computational forensic study

as far as reconstruction is concerned. Essentially, it is to reconstruct the dynamic process based upon a known cause (an explosion) and resulting outcome (a definable hole in the side of the airframe). Moreover, any inadequacy or incorrectness in the existing modeling and computation can be clearly observed, then rectified or improved by our understanding of the incident itself or, in other words, the known factors.

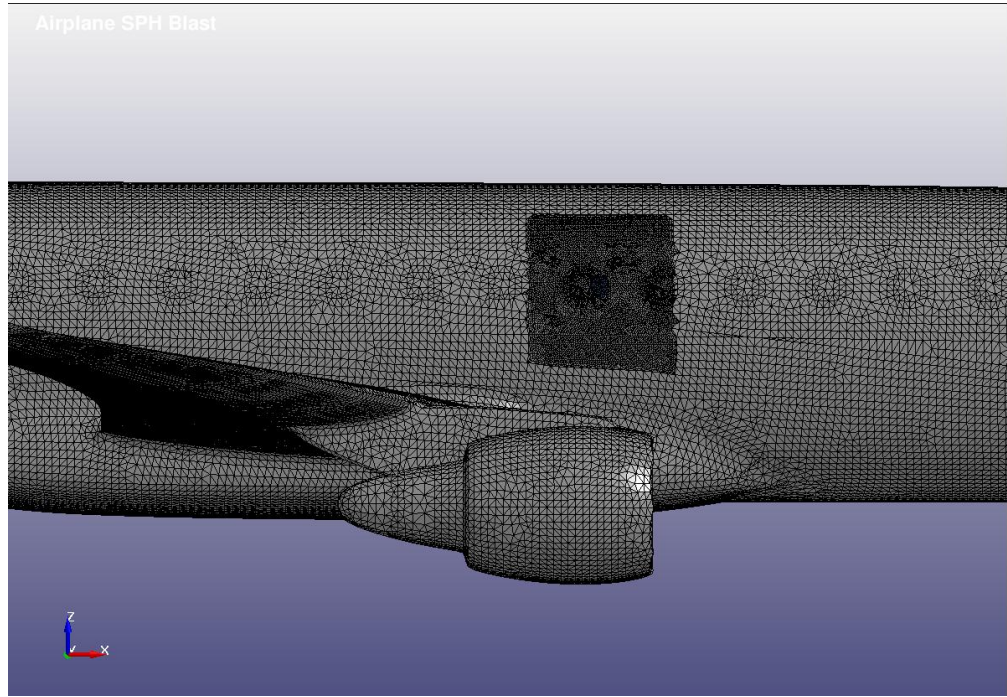
5.1 Bombing of a “Base Model” of an Airbus A321 Airliner

The airplane of Daallo Flight 159 is an Airbus A321-111, SX-BHS, model. We found the aircraft information about model A321 online at [15, 16]. A finite element mesh was generated by using LS-PREPOST [9]. See Figure 5.1. Inside the fuselage, we have also put in a plastic wall. This constitutes our “base model” of the airplane.

The explosives and the air particles are modeled by SPH [8, Theorey Manual, p.38.1]. As noted in Box 1, the air pressure difference between the inside and the outside of the cabin is set to be 8 psi, which is about equal to that for an aircraft at the altitude of 11,000 ft. A volume of $24 \times 1.5 \times 24 \text{ cm}^3$ TNT (1.43 kg) is placed near the wall above and close to the right wing end of the aircraft. We now set the TNT charge to explode. The outcome can be seen in Figure 5.2 parts (b) and (c), which can be compared with the actual aircraft damage in the photograph of Figure 5.2(a).



(a)



(b)

Figure 5.1: Finite element mesh generation of an Airbus A321 model aircraft by LS-PREPOST. The aircraft is assumed to be made of thin shell with uniform thickness 1.2 mm, based on [17]. There are a total of 158709 finite elements.

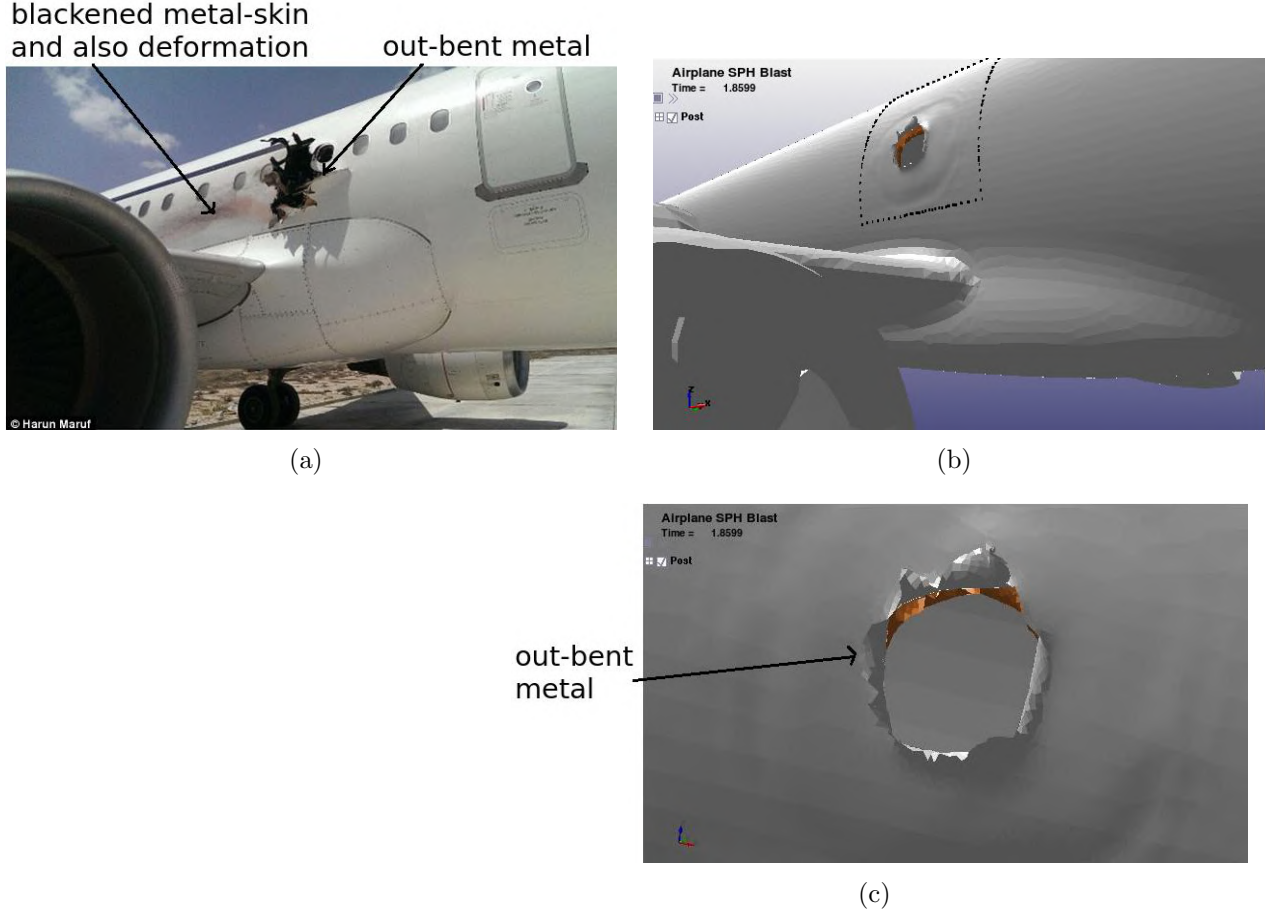


Figure 5.2: Comparison between the real airplane damage to Daallo Flight 159, part (a), and the simulation results, part (b) and (c), where $24 \times 1.5 \times 24 \text{ cm}^3$ TNT is used for a base model Airbus A321 aircraft. For the computed damage to the fuselage, one can clearly see that the metal is bent outward onto itself, in a pattern identified as (**P1**) in Section 2 of this paper.

We note that no precise information was found concerning the identification of a specific type of explosive the terrorist has used in the bombing - logically, it would be a *moldable* explosive such as C-4, Semtex or a PETN-based sheet explosive (rather than TNT) so it could fit into a laptop. The amount of TNT in our computer simulations should be regarded as *TNT equivalent* explosives.

What can Figure 5.2 tell us in a forensic investigation? There are good news and bad news:

- (1) The size and dimension of the blown-up hole from computation is consistent with that suffered by the actual airplane. It clearly manifests the bombing characteristic (**P1**) in Section 2.
- (2) The fine details between the two damaged holes (in Figure 5.2, parts (a) and (b)) differ. The real one is somewhat “square” in shape, while the computed one is more “round”.

Also, the former is larger in size.

Can we reconcile the differences in (2) above? The solution requires *refinement of the base model*; see the next subsection.

5.2 Refinement of the Airplane Model with Rings, Stringers and Windows

When we first investigated the computational results, we were baffled by the somewhat *square shape* of the hole damage on the airliner.

After a broad Internet search, we have found two photos of the interior damage to the airliner; see Figure 5.3. These photos clearly show that the blown-up hole is confined by the two thick stations (on the left and right) and two stringer (at the top and bottom).

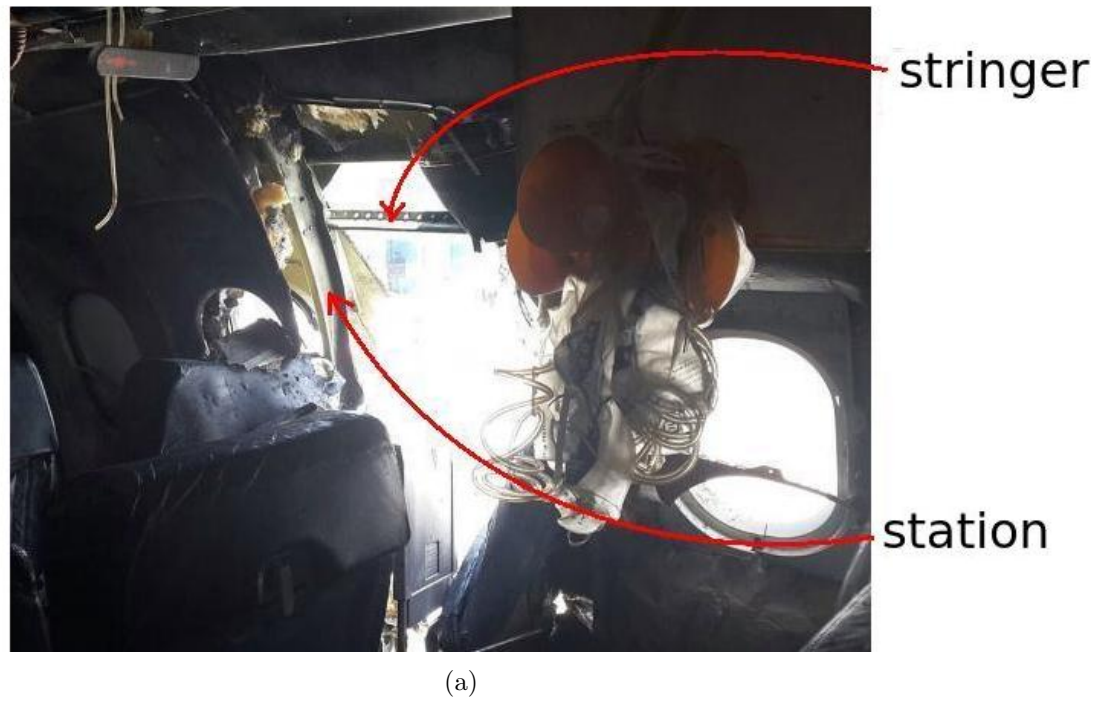
The observation from Figure 5.3 is instructive: it clearly indicated that the *forensic assessments of bomb damage will not be accurate unless stations, stringers and windows are taken into account in the mathematical and computational model*.

Therefore, we add the following features in the airplane model:

- (1) four stations: made of aluminum alloy (model 2024-T4);
- (2) two size 31.2 cm × 23 cm acrylic windows.

See Figure 5.4. Note that earlier, we have already built in a plastic wall in the inside of the fuselage. For the information regarding the merging of windows with the fuselage and the attachment of the stations, see Box 1 for the LS-DYNA software subroutines involved.

Now, we can set the TNT (equivalent) explosive charge, in the amount of 0.35208 kg, to explode. See the video animation given in the captions of Figure 5.5.



(a)



(b)

Figure 5.3: The photos show the interior damage of the Daallo airliner after the blast. It is noteworthy that the blown-up hole is essentially confined within the two stations and two stringers. Such stations and stringers provide a strong protective effect to the airframe, causing the damaged hole to take a nearly square shape.

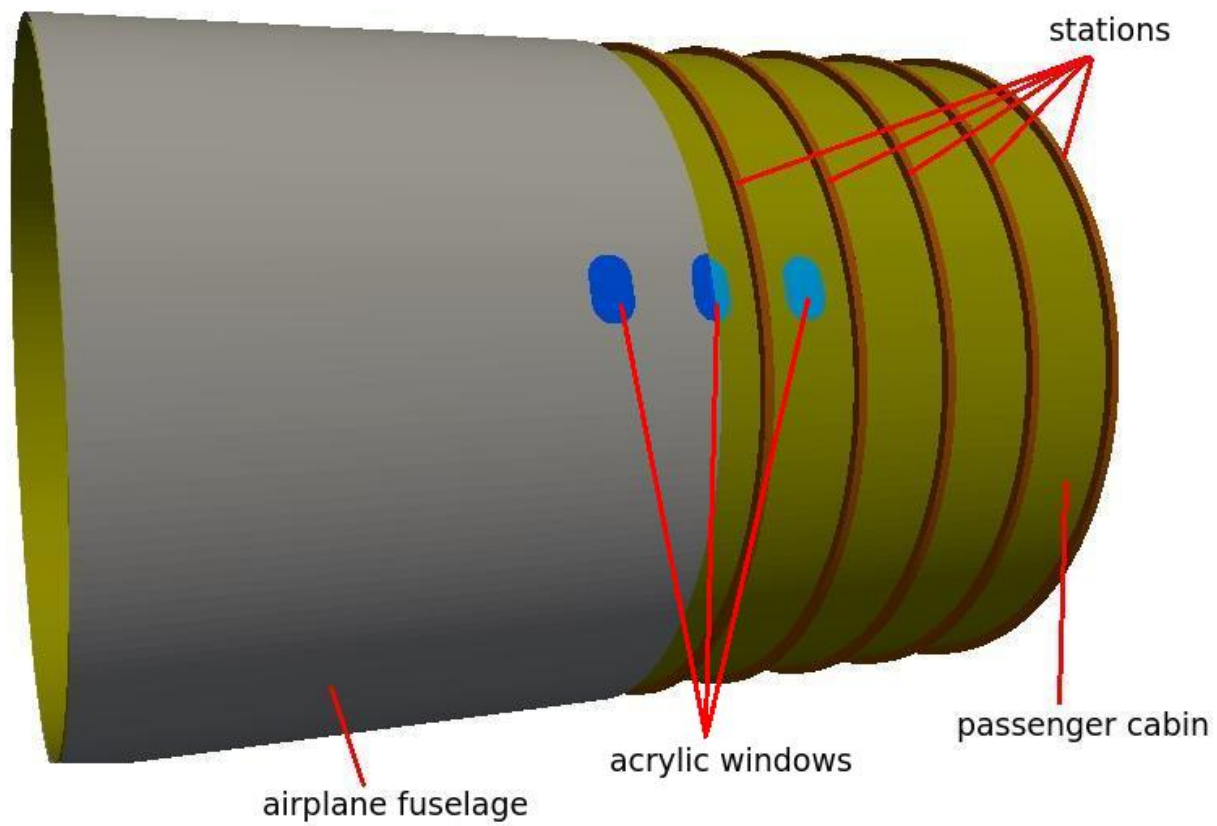


Figure 5.4: A refined model of the Airbus A321 aircraft. The stations and three acrylic windows have been added.

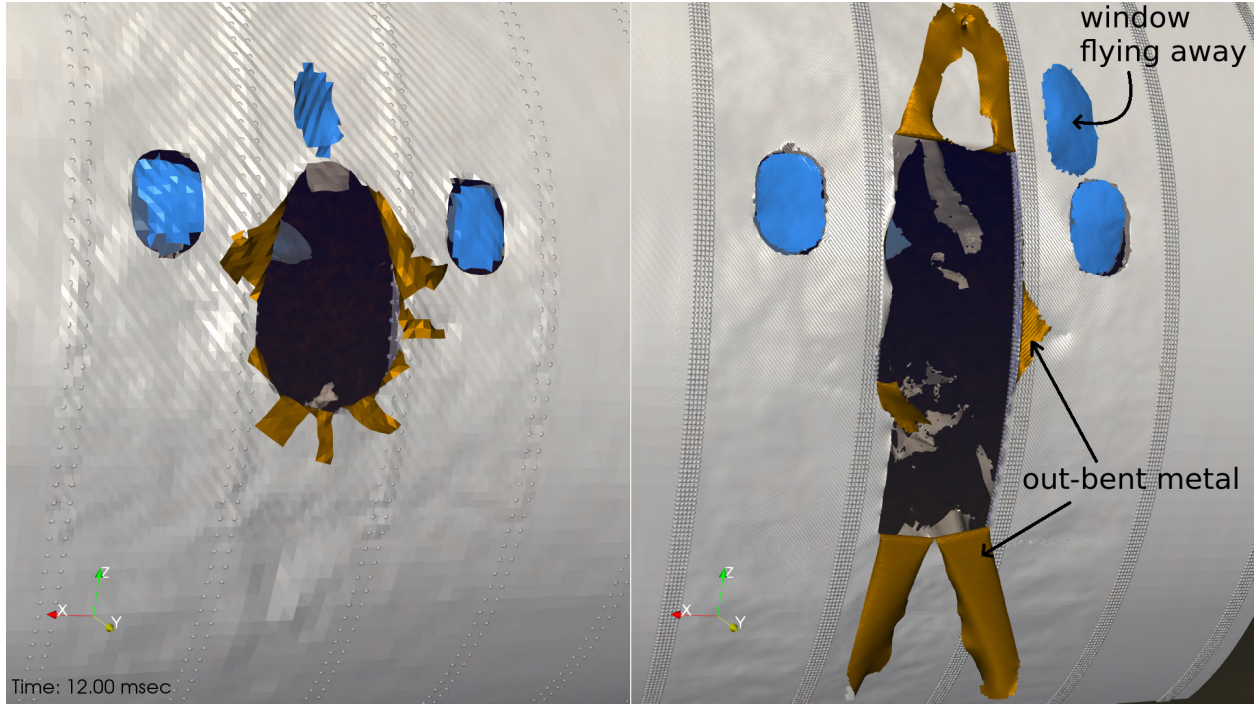


Figure 5.5: This figure contains two parts. The left, part (a), is computed from a cruder finite element mesh, while the right, part (b) used a finer mesh. An amount of TNT explosive 0.35208 kg is used in the computations. For video animations, see <https://www.dropbox.com/s/fankgolhu7wo2o8/fuselage.mp4>. The bombed hole in part (b) takes the shape like a square very much like the reality case, as the one shown in the photo of Figure 5.2(a). It is also interesting to note, from the video animation, that the acrylic window in parts (a) and (b) broke off and flew away, in one piece (rather than shattered).

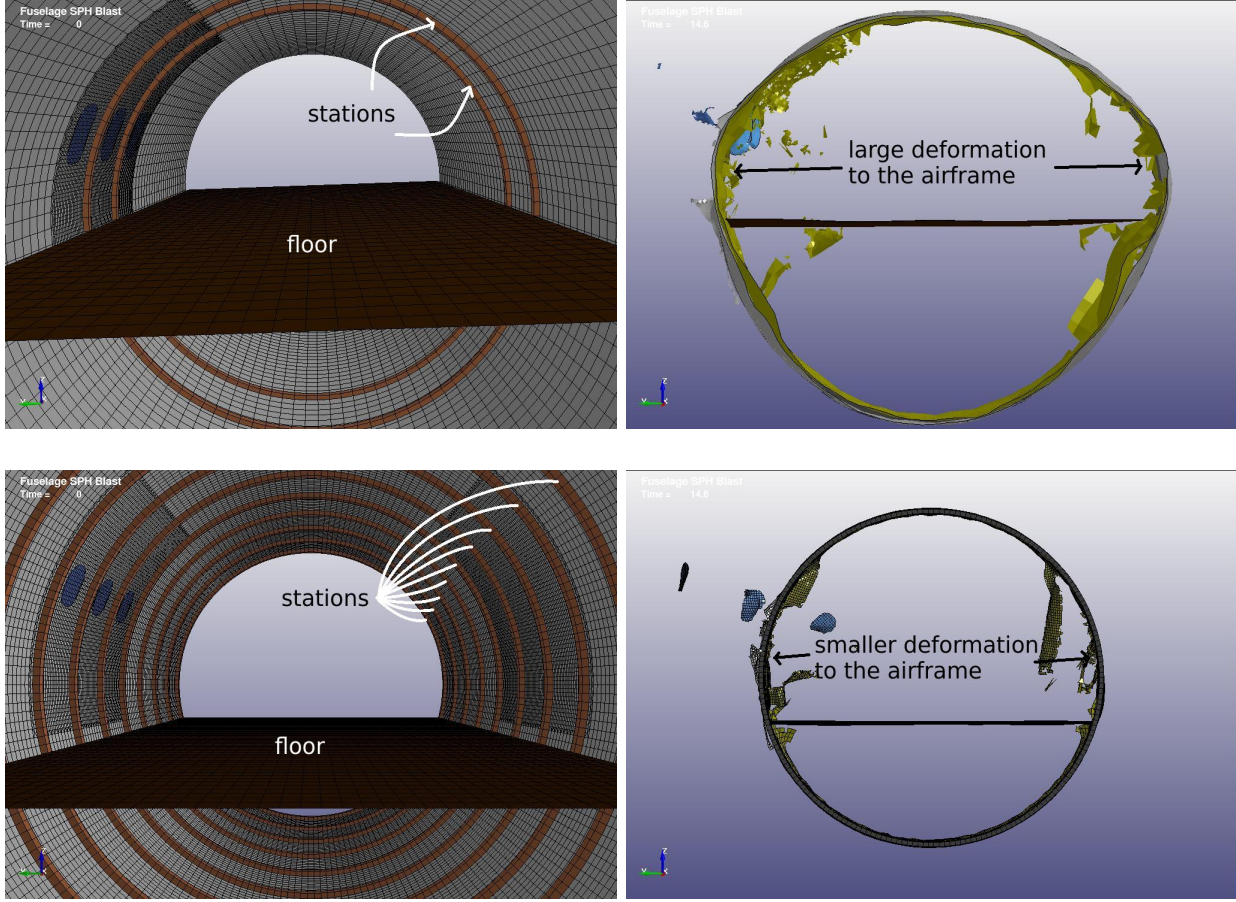


Figure 5.6: The top two panels are the cabin fuselage with only two stations and the bottom two are the one fully supported by more stations. The left two show the setting of the stations, and the right two are the results of damage after 14 ms of blast. One can clearly see that the inclusion of more stations can help protect the fuselage against distortion.

One can see that the final damage-hole on the aircraft body is now nearly square in shape with bent metal on the rim, whose size is quite consistent with the real damaged aircraft photo in Figure 5.2, part (a).

Therefore, our animation video

<https://www.dropbox.com/s/fankgolhu7wo2o8/fuselage.mp4> (5.1)
serves as a good *event reconstruction* for this Daallo Flight 159 bombing. Our estimated explosive (TNT equivalent) amount used by the terrorist is 0.35208 kg.

Figure 5.5 has shown some *local* damage to the aircraft. Now we also illustrate some *global* damages. In Figure 5.6, left column, we show two segments of the airframe: the upper one has only two stations built in, whereas the lower one has eight. Both settings also have floors. After detonating the same amount explosive of 0.35 kg TNT, at 14 ms, we can see that the deformation damage to the airframe is greater in the upper panel than that in the lower panel. This clearly shows the *protective effects of supporting stations against a limited amount of bomb blast*.

6 Concluding Remarks

In any forensic investigation on bombing, there are several important issues to address, do and examine. What we have done are:

- (i) *Event reconstruction*: this has been achieved by us in (5.1);
- (ii) *Determine the types of explosives used*: this can only be done by field investigation work and on-site collected samples and evidences and is, therefore, beyond the scope of computational mechanics alone;
- (iii) *Determine the amount of explosives used*: this we have computed and simulated to be approximately 0.35 kg of equivalent TNT;
- (iv) *The location of bomb placement*: This is more or less clear from the location of the bomb-damaged hole near where the bomber was seated on the airplane. In our computations, we use the following configuration:

Positioning of the bomb is shown as in Figure 6.1, which shows the arrangement of almost complete contact of the bomb with the acrylic window in the mind-set of the bomber (hoping to maximize the bomb damage). (By varying the orientation of the laptop bomb, we did not find much differences between the outcomes of bomb damages.)

Consequently, the contributions of our forensic analysis in this paper lie primarily in items (i) and (iii) above.

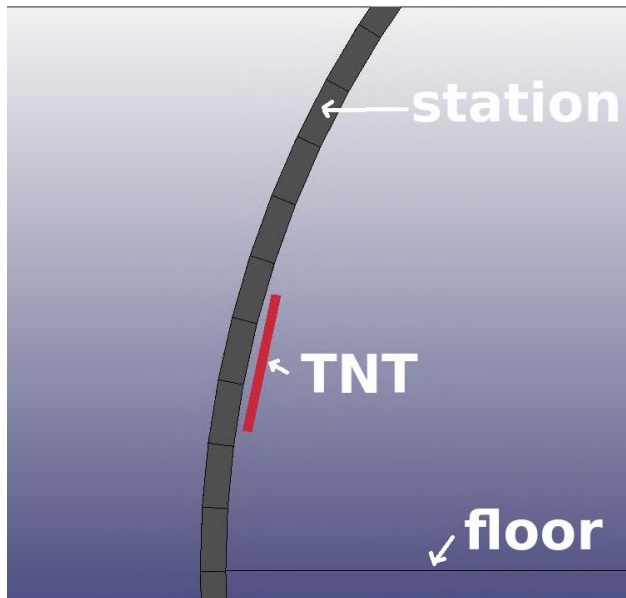


Figure 6.1: The positioning of the laptop bomb in the airplane of Daallo Airlines Flight 159. We assume that the bomb is arranged in almost complete contact with the window.

The work being studied in this paper has the flavor of *fluid-structure interactions* where the fluid is the ambient air while the structure is that of the airplane. Thus, one expects CFD + FEM (computational fluid dynamics + finite element method) approach as the standard way to treat such a problem. Nevertheless, our ingredients and methodology has gone beyond CFD + FEM - it is now

$$\text{CFD} + \text{FEM} + \text{Blast} + \text{SPH}$$

, where there is a milli-second, fast reacting explosion process. We have also incorporated SPH (smoothed particle hydrodynamics), see Box 1 as part of our innovative contributions in order to be able to enhance the visualization of the debris-splattering effects of explosion

Airliner bombings occur infrequently. However, their forensics investigation methodology needs to be researched and developed. Based on evidential bombing characteristics (Section 2) and mathematical/computational modeling and validation (Section 3), we hope our work here has provided a sound foundation for this important field. Many issues, such as the construction of even more refined models for the aircraft, and to quantify and capture bombing phenomena with fine details, remain to be done. Furthermore, the important aspect of *de-compressive explosion*, which is extremely important in high-altitude cruising flight, has not been modeled and computed due to our current limited expertise. These will constitute interesting work and challenges for the future.

7 Acknowledgements

We thank Texas A&M University's High Performance Research Computing Center for technical assistance and for generous allocation of hours. The work of G. Chen in supported in part by Qatar National Research Fund Grant #NPRP 9-166-1-031.

References

- [1] J. A. Zukas and W. Walters, *Explosive Effects and Applications*. Springer-Verlag New York, 1998.
- [2] R. Forsen, "Experiments used for comparison of blast damage to full-scale and one fourth scale reinforced concrete structures.", tech. rep., 24th DoD Explosives Safety Seminar, Saint Louis, MO, 1990.
- [3] J. Yeh, *Computational Mechanics for Shape Optimization and Airplane Bombing Based on OpenFOAM and LS-DYNA Software*. PhD thesis, Department of Mathematics, Texas A&M University, College Station, TX, USA, 12 2018.
- [4] J. T. Thurman, *Practical Bomb Scene Investigation*. Practical Aspects of Criminal and Forensic Investigations Series, Boca Raton, FL: CRC Press, Taylor & Francis, third edition ed., 2017.

- [5] Wikipedia contributors, “Pan am flight 103 — Wikipedia, the free encyclopedia.” https://en.wikipedia.org/wiki/Pan_Am_Flight_103/.
- [6] R. A. Marquise, *Scotbom: Evidence and the Lockerbie Investigation*. New York, NY: Algora Publishing, 2006.
- [7] Livermore Software Technology Company, “LS-DYNA.” <http://www.lstc.com/products/ls-dyna>.
- [8] Livermore Software Technology Company, “LS-DYNA manuals and theory manual.” <https://www.dynasupport.com/manuals>.
- [9] Livermore Software Technology Company, “LS-PrePost.” <http://www.lstc.com/products/ls-prepost>.
- [10] ParaView Contributors, “ParaView.” <https://www.paraview.org>.
- [11] D. L. Shirey, “Breaching of structural steel plates using explosive disks,” tech. rep., The Shock and Vibration Bulletin, 1980.
- [12] L. Lonnqvist, “The effects of high explosives in contact with reinforced concrete slabs,” tech. rep., Proceedings of the Sixth International Symposium on Interaction of Nonnuclear Munitions with Structures, Panama City Beach, FL., 1993.
- [13] Simon, “Fuselage boeing — GrabCAD Community.” <https://grabcad.com/library/fuselage-boeing-1>.
- [14] Wikipedia contributors, “CATIA 3D software — Wikipedia, the free encyclopedia.” <https://en.wikipedia.org/wiki/CATIA/>.
- [15] E. T. Academy, “A320 family.” <http://training.egyptair.com/Maintenance/A320Family>.
- [16] Airbus, “A320.” <http://www.airbus.com/aircraft/passenger-aircraft/a320-family/a321neo.html>.
- [17] AirBUS, “Flight airworthiness support technology — FAST33.” <https://www.airbus.com/content/dam/corporate-topics/publications/fast/FAST33.pdf>.